Sidelobe Suppression in Pulse Compressed Radar Signals

Mrignedra Kumar

Department of Electronics & Communication Engineering
National Institute of Technology Rourkela

Sidelobe Suppression in Pulse Compressed Radar Signals

A Dissertation submitted in Partial Fulfilment

of the Requirements for the Degree of

Master of Technology

In

Electronics & Communication Engineering

(Specialization: Signal And Image Processing)

by

Mrigendra Kumar

(Roll No: 214EC6427)

based on research carried out
under the supervision of

Prof. Ajit Kumar Sahoo

May, 2016

Department of Electronics and Communication Engineering

National Institute of Technology Rourkela

Department of Electronics & Communication Engineering
National Institute of Technology Rourkela

May 27, 2016

Certificate of Examination

Roll Number: 214EC6427

Name: Mrigendra Kumar

This is certify that the thesis entitled *"Sidelobe Suppression in Pulse compressed Radar Signals"*, being submitted by *Mrigendra Kumar*, Roll No. 214EC6427, to the National Institute of Technology, Rourkela for the award of the degree Master of Technology in Electronics & Communication Engineering, is a bonafide record of research work carried out by him under supervision and guidance of *Prof. Ajit Kumar Sahoo*.

The candidate has fulfilled all the prescribed requirements.

We the below signed, after checking the project report mentioned above and the official record book of the student, hereby state our approval of the dissertation submitted in partial fulfilment of the requirements of the degree of Master of Technology in Electronics & Communication Engineering, at National Institute of Technology Rourkela. We are satisfied with the volume, quality, correctness, and originality of the work.

Supervisor

Prof. Ajit Kumar Sahoo

Assistant Professor, Department of Electronics & Communication Engineering

Department of Electronics & Communication Engineering
National Institute of Technology Rourkela

May 27, 2016

Prof. Ajit Kumar Sahoo
Assistant Professor

Supervisor's Certificate

Roll Number: *214EC6427*

Name*: Mrigendra Kumar*

Title of Dissertation: *Sidelobe Suppression in Pulse compressed Radar Signals*

We the below signed, after checking the dissertation mentioned above and the official record book (s) of the student, hereby state our approval of the dissertation submitted in partial fulfilment of the requirements of the degree of *Master of Technology* in *Electronics & communication* at *National Institute of Technology Rourkela*. We are satisfied with the volume, quality, correctness, and originality of the work.

Prof. Ajit Kumar Sahoo

Dedication

To my Family, Friends and The Almighty.

Declaration of Originality

I, *Mrigendra Kumar*, Roll Number *214EC6427* hereby declare that this dissertation entitled *Sidelobe Suppression in Pulse Compressed Radar Signals* presents my original work carried out as a M. Tech student of NIT Rourkela and, to the best of my knowledge, contains no material previously published or written by another person, nor any material presented by me for the award of any degree or diploma of NIT Rourkela or any other institution. Any contribution made to this research by others, with whom I have worked at NIT Rourkela or elsewhere, is explicitly acknowledged in the dissertation. Works of other authors cited in this dissertation have been duly acknowledged under the sections "Reference" or "Bibliography". I have also submitted my original research records to the scrutiny committee for evaluation of my dissertation.

I am fully aware that in case of any non-compliance detected in future, the Senate of NIT Rourkela may withdraw the degree awarded to me on the basis of the present dissertation.

May 27, 2016
NIT Rourkela

Mrigendra Kumar

Acknowledgment

The real spirit of achieving a goal is through the way of excellence and austere discipline. I would have never succeeded in completing my task without the cooperation, encouragement and help provided to me by various personalities.

I am grateful to numerous local and global peers who have contributed towards shaping this thesis. At the outset, I would like to express my sincere thanks to Prof. Ajit Kumar Sahoo for his advice during my thesis work. As my supervisor, he has constantly encouraged me to remain focused on achieving my goal. His observations and comments helped me to establish the overall direction of the research and to move forward with investigation in depth. He has helped me greatly and been a source of knowledge.

I must acknowledge the academic resources that I have got from NIT Rourkela. I would like to thank administrative and technical staff members of the Department who have been kind enough to advise and help in their respective roles.

I am really thankful to my all friends. My sincere thanks to everyone who has provided me with kind words, a welcome ear, new ideas, useful criticism, or their invaluable time, I am truly indebted.

At last, I would conclude with my deepest gratitude to my parents, my classmates and all my loved ones. My full dedication to the work would have not been possible without their blessings and moral support. This thesis is a dedication to them who did not forget to keep me in their hearts when I could not be beside them.

May 27,2016 *Mrigendra Kumar*

NIT Rourkela Roll Number: 214EC6427

Abstract

Radio Detection And Ranging, RADAR, is a system that is used to detect and track a target at distant location with its other features (like velocity, direction etc.). The system uses various techniques to enhance its efficiency in terms of different physical parameters. Pulse compression technique provides the radar designers with an ability to combine the benefits of low power transmitters and the larger pulse wavelength to maintain the energy content of the pulse, in turn, the process elevates the range detection ability of high duration pulses and the resolution capacity of short pulses. To enhance the bandwidth of the high duration pulses so that better range resolution capability can be achieved, modulation in frequency and phase is done. Frequency or phase modulation is employed to a long duration pulse before it is transmitted and the received pulse is then passed through a filter to get its energy accumulated into a short pulse.

Usually, matched filter is a common choice for pulse compression. Due to the high sidelobe peaks associated with the mainlobe in the matched filter output, which is simply an ACF of the input pulse, they have the possibility of masking the weaker targets near the stronger ones. So, the high sidelobes are needed to be suppressed to avoid such circumstances. Normally, the matched filter output has the sidelobe level of -13.5dB which can be improved by the use of the techniques like adaptive filtering, weighting through the use of windows etc. The windowing technique, besides suppressing the sidelobe also reduces the SNR which leads to reduction in rate of false alarm rate. A stepped frequency train of LFM pulses is an efficient method to enhance the overall bandwidth of the signal and maintaining the instantaneous bandwidth at the same time. But they are associated with the ambiguous peaks whose peak value is similar to the mainlobe peak and are also known as the grating lobes which have the potential of masking the smaller targets. So, it becomes necessary to suppress or nullify them by proper adjustment of the design parameters.

Keywords: ***Pulse compression, Barker code, LFM, PSLR, ACF, AF***

Content

List of Figures

Chapter 1

Introduction

1.1 Background

RADAR, that is, Radio Detection and Ranging is a system, based on the principle of electromagnetism used to detect and locate the distant objects like aircraft, ships, vehicles, missiles etc. It works on the theory of transmission of energy in space and reception of the reflected echo from the distant object. It can work in any physical conditions like rain, snow, fog, darkness etc. The technology has got its initiation during the World War II. And, the post war period had seen a tremendous development in its features [1].

The ability to detect the target and its respective features like range, velocity etc. in all weather conditions with greater accuracy is its most important feature. Its antenna and tracking system play an important role in determining the target's angle and direction from the echo obtained from the target after getting reflected from it [1],[2]. The range of the target is the function of the delay in the reception of the transmitted pulse whereas the target's velocity is the function of the Doppler shift of the received signal.

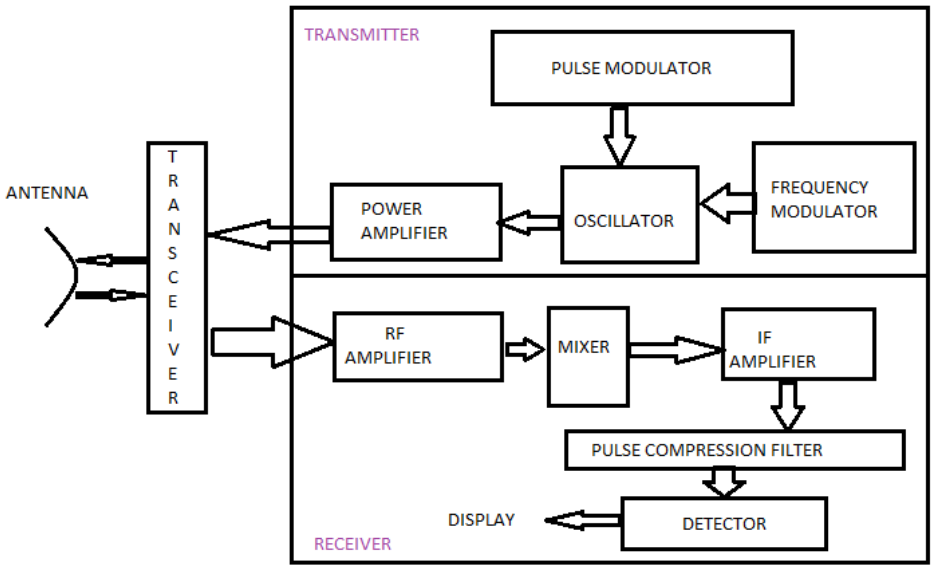

Figure 1. Pulse Compression System

Though the peak power of the transmitted pulse is generally in megawatts, it keeps on increasing high and high so that the range detection can be enhanced. This increase in the transmitted peak power imposes economic burden as well as technical limitation. Even with the increase in power the accuracy and the target resolution become repugnant. It was Siebert who found out that range to which a radar can detect the target is associated only

with the ratio of the energy of the received signal to that of the power spectral density of the noise and is quite independent of the waveform [3]. This is why, most of the radar designers have shifted their endeavor from designing of the transmitters with high power to the design of the pulses with higher duration so that the requirements of the range resolution and accuracy can be fulfilled.

So, radar signal processing integrates various attributes of the transmitted waveforms with radars, performance evaluation, detection theory and the connected circuitry to the displays and antenna or the processing units involved. The radar design to signal processing is similar to the communication system to the modulation theory, where both strive to achieve better communication so that maximum information can be extracted and the effects of the noise or interference can be minimized

Out of various components of the radar system development, waveform design is an important part. Waveform used in radar systems play pivotal role in determination of the range resolution and the maximum detection capability (detection range) of the radar [4]. Range resolution is defined as the ability to separate two closely placed targets with different ranges but with same bearing angle, which has inverse proportionality with the bandwidth of the transmitted signal i.e. the signal with higher bandwidth has better range resolution than the signal with low bandwidth [1]. The mathematical relation between the range resolution and the corresponding bandwidth is:

$$R_r = \frac{C}{2B} \tag{1.1}$$

Here, C is the velocity of the light and B is the signal's bandwidth.

Also, for a signal with pulse duration of T and without modulation, the bandwidth is given by:

$$B = \frac{1}{T} \tag{1.2}$$

A signal with short pulse duration will have higher bandwidth and hence has a better (high) range resolution, thus finds an important place in various radar applications. But, the short pulse duration signals have limitations too. As the signal's bandwidth is inversely proportion to the pulse duration, the short pulse have higher bandwidth. And, the high bandwidth signals make the systems very complex. Also, short duration pulses requires more peak power so that it can furnish enough energy required for its transmission to far distances. Now, to generate the short pulses with very high peak power, it requires high

power receivers and transmitters which are very difficult to design as the components have to withstand high power.

This is a serious problem to sort out. One way to enhance the energy of the short pulses is by modulating the short pulses into longer ones so that the bandwidth of the longer pulses can be enhanced lest the resolution capacity of the radar system should not be compromised and the technique that is employed to achieve this goal is termed as the Pulse Compression [3], [9]. This technique is of immense use in the radar application where it is undesirable to use high peak power.

In 1950s, the radars had been developed practically with the technology called pulse compression. The technique comprises of the transmitted signal having phase modulated or frequency modulated and the signal after reception is processed through the matched filters [5], [6]. Initially, it was tough to realize the matched filters with the help of traverse filters as there is a lack of delay line having enough bandwidth. Recently, there are many refined filters used instead of the matched filters.

1.2 Pulse Compression

The energy in the transmitted pulse(signal) should be high lest the received reflected echo must have the sufficient energy as the maximum detection range of the radar depends on the strength of the received pulse(echo). The transmitted pulse gets attenuated by the environmental factors in the course of its transmission before and after being reflected from the target. The energy of the pulse is determined by the product of the peak power and the duration of the corresponding pulse. The short duration pulse with high peak power has the equivalent energy as that of the pulse with high pulse duration and low peak power. Achieving high peak power requires complicated hardware setup and also the cost of the setup goes high.

Thus, a transmitted pulse should be a low peak power pulse with long duration to enhance the range detection capability of the radar but at the receiver end it requires to be a pulse of short duration so that the range resolution capability should get refined [7]. As the range resolution of the radar is given by the relation, $R_r = \frac{C}{2B}$, where B and C are the bandwidth of the transmitted pulse and velocity of the light.

Now, to amalgamate the advantages of the high range resolution capability of the short duration pulse, as they have higher bandwidth, and the high detection range capability of the long duration pulse, as they have high energy, the process of pulse compression is used

[8], [10]. Generally, the modulation techniques like frequency and phase modulation techniques are used to achieve the goal of higher bandwidth so that the range resolution is enhanced. The modulation techniques are applied to the long duration pulses prior to their transmission and the reflected echo, after reception, is processed in the matched filter that agglomerates the energy of the echo into a very small time duration.

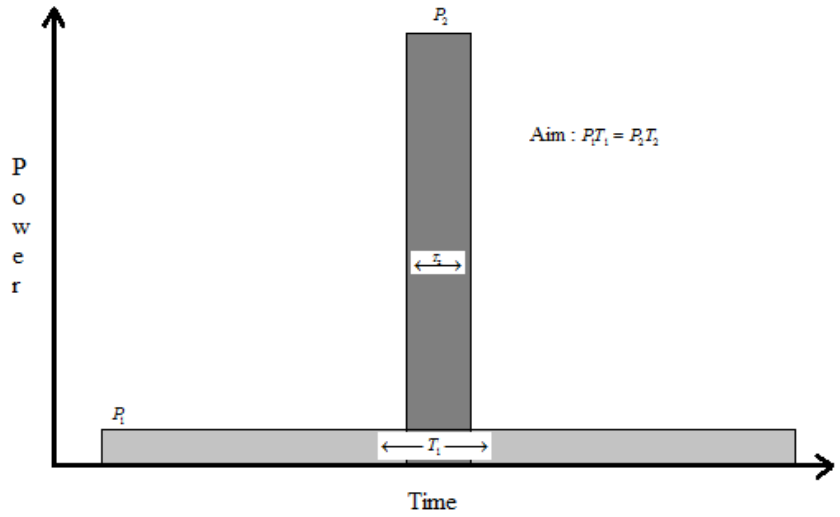

Figure 2. Plot showing pulses with different duration and same energy

The measure of the compression with respect to the uncompressed pulse is represented in terms of the factor called Pulse Compression Ratio (PCR) [1].

$$PCR = \frac{Pulse\ Width\ Before\ Compression}{Pulse\ Width\ After\ Compression} \tag{1.3}$$

The PCR is the figure of merit of the pulse compression system which is equal to the Time-Bandwidth product (TBWP) of the signal.

1.3 Matched Filter

The target's features are extracted from the received reflected pulse in the radar processing. As obvious, the reflected echoes are highly affected by the noise. The most exclusive feature of the matched filter is that it maximizes the achievable SNR at its output when a corrupted signal(with additive white noise) is given as its input. Higher is the SNR, higher will be the probability of detection of the respective target by the radar. Thus, as pointed out by Siebert [3], it becomes necessary for the radar system to maximize the energy of the received pulse by maximizing the SNR rather perpetuating the signal's shape. The matched filter is quite apt to be used at the receiver's side of the radar system as it has the property of accumulating the energy of the input signal, which is here the received echo from the target, by matching

the receiver's transfer function to that of the received pulse. Experiments have shown that regardless of the waveform used the output of the matched filter is always twice the ratio of the energy of the input pulse to the noise power [2]. The transmitted pulse with the Additive White Gaussian Noise(AWGN) becomes the input to the matched filter as shown in the block diagram . The white noise has the power spectral density of $\frac{N_0}{2}$. The input for the matched filter can be represented by:

$$x(t) = s_i(t - t_1) + n_i(t) \tag{1.4}$$

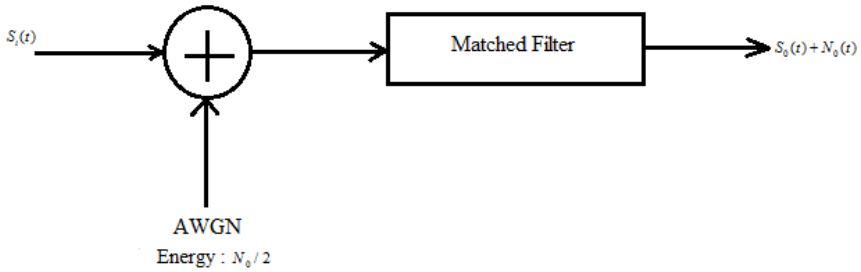

Figure 3. Block Diagram for Matched Filtering

where, t_1 being the time delay proportional to the target's range and $n_i(t)$ is the input white noise whose corresponding autocorrelation and Power Spectral Density is given by:

$$R_{n_i}(t) = \frac{N_0}{2}\delta(t) \tag{1.5}$$

$$S_{n_i}(\omega) = \frac{N_0}{2} \tag{1.6}$$

where, N_0 is constant.

Now, the output of the matched filter can be descripted as:

$$y(t) = s_o(t - t_1) + n_o(t) \tag{1.7}$$

where,

$$s_o(t) = s_i(t) \otimes h(t) \tag{1.8}$$

$$n_o(t) = n_i(t) \otimes h(t) \tag{1.9}$$

here, $\otimes$ denotes the convolution and $h(t)$ is the impulse response of the matched filter. And the filter is assumed to be time invariant and linear [2].

From (3) and (4), and assuming $R_m(t)$ to be the matched filter autocorrelation function, the autocorrelation of the output noise is given by:

$$R_{n_o}(t) = R_{n_i}(t) \otimes R_m(t)$$

$$= \frac{N_0}{2}\delta(t) \otimes R_m(t)$$

$$= \frac{N_0}{2} R_m(t) \tag{1.10}$$

And, the Power Spectral Density of the output noise is given by:

$$S_{n_o}(\omega) = S_{n_i}(\omega)\left|H(\omega)\right|^2$$

$$= \frac{N_0}{2}\left|H(\omega)\right|^2 \tag{1.11}$$

where, $H(\omega)$ is the Fourier transform of the filter impulse response, $h(t)$.

More precisely, the total average output noise power, evaluated at $t = 0$, is given by:

$$R_{n_o}(0) = \frac{N_0}{2}\int_{-\infty}^{+\infty}\left|h(u)\right|^2 du \tag{1.12}$$

The output signal of the matched filter is given by:

$$s_0(t - t_1) = \int_{-\infty}^{+\infty} s_i(t - t_1 - u)h(u)du \tag{1.13}$$

The aim is to design the filter with such impulse response that maximizes the output SNR i.e.

$$SNR(t) = \frac{\left|s_o(t - t_1)\right|^2}{R_{n_o}(0)} \tag{1.14}$$

Substituting Eq. (11) and (12) in the (13), will become,

$$SNR(t) = \frac{\left|\int_{-\infty}^{+\infty} s_i(t - t_1 - u)h(u)du\right|^2}{\frac{N_0}{2}\int_{-\infty}^{+\infty}\left|h(u)\right|^2 du} \tag{1.15}$$

Now applying Schwartz inequality and simplifying the expression (14), we get:

$$SNR(t) \le \frac{\int_{-\infty}^{+\infty}\left|s_i(t - t_1 - u)\right|^2 du \int_{-\infty}^{+\infty}\left|h(u)\right|^2 du}{\frac{N_0}{2}\int_{-\infty}^{+\infty}\left|h(u)\right|^2 du}$$

$$\leq \frac{2\int_{-\infty}^{+\infty} |s_i(t-t_1-u)|^2 \, du}{N_0} \tag{1.16}$$

which is valid only under the condition, $h(u) = k \cdot s_i^*(t_0 - t_1 - u)$, and k can be taken as equal to 1. Thus the maximum SNR will be:

$$SNR(t_0) = \frac{2\int_{-\infty}^{+\infty} |s_i(t-t_1-u)|^2 \, du}{N_0} \tag{1.17}$$

which can be further simplified using Parseval's theorem into,

$$E = \int_{-\infty}^{+\infty} |s_i(t-t_1-u)|^2 \, du \tag{1.18}$$

where, E is the energy of the input signal to the matched filter. Hence, the expression for the SNR of the output signal of the matched filter will become:

$$SNR(t_0) = \frac{2E}{N_0} \tag{1.19}$$

Hence, it can be concluded that the peak instantaneous SNR is dependent only on the signal energy and the input noise power and is independent of the waveform utilized by the radar system.

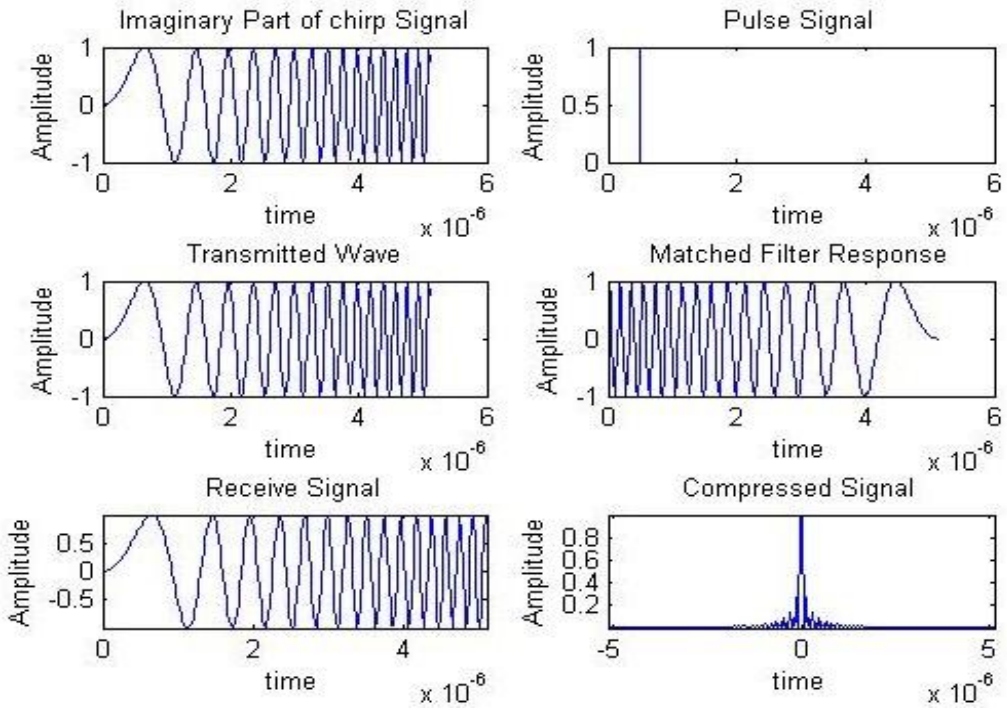

Figure 4. Plot showing compressed chirp signal using matched filter with zero delay

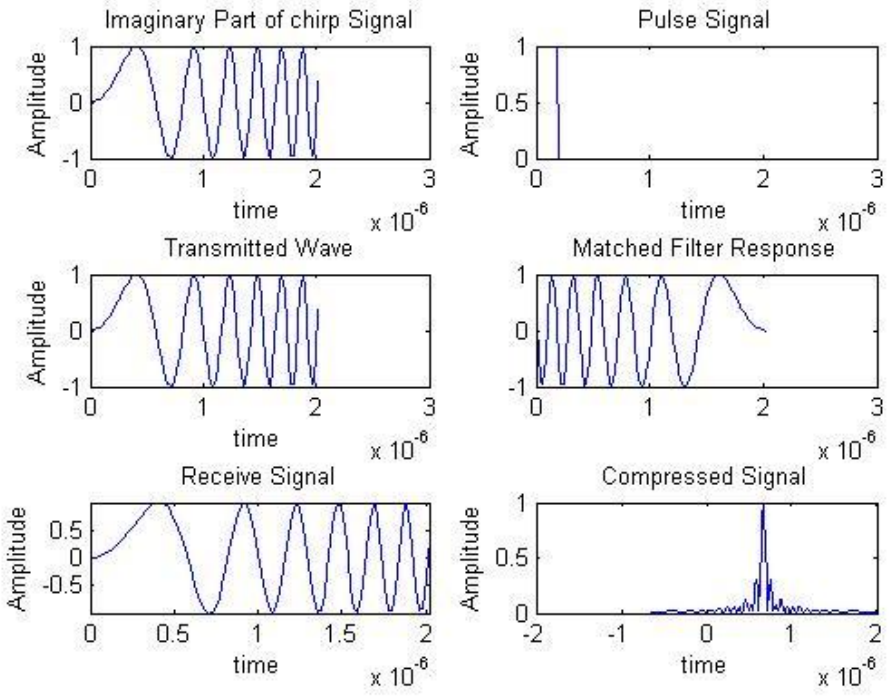

Figure 5. Plot showing compressed chirp signal using matched filter with delay of 100 samples

1.4 Ambiguity Function

The ambiguity function of the radar is used to examine different waveforms. It provides an insight to the designer that how various waveforms are suitable for different applications in the radar system. The radar ambiguity function is used to represent the matched filter output. It denotes the interference caused by the range and Doppler shift of the target when compared to the reference target of equal radar cross section [1]. It gives the range and the Doppler resolution for the given radar waveform. While detecting closely placed targets with varying radial velocity, the radar receiver's filter are matched not only to the transmitted signal but also with the various Doppler shifted versions of the signal lest the targets with different radial velocity can be uniquely identified. In these kind of cases, the different targets will produce the peaks at different Doppler shifted matched filter and hence it becomes necessary to examine the output of the matched filter in two different dimensions i.e. the time delay, τ , and the Doppler shift, ν . Precisely, the ambiguity function expresses the output of a matched filter when a signal with finite energy having a time delay of an interval τ and a Doppler shift of ν is passed through it, as compared to the expected values of the filter's matched response. Mathematically, it is denoted as [1]:

$$\left|X(\tau,\nu)\right|^2 = \left|\int_{-\infty}^{+\infty} s(t)s*(t+\tau)e^{j2\pi\nu t}dt\right|^2 \tag{1.20}$$

where, $s(t)$ is the signal's complex envelope. τ being positive means that the target is farther from the radar and for the Doppler shift, ν, being positive means the target is moving towards the radar and being negative means that the target is moving away from the radar. The ambiguity function is the mathematical tool for analyzing the radar waveform behavior [11].

1.3.1 Ambiguity Function Characteristics

The ambiguity function has the following characteristics [1], [11]:

A. The ambiguity function has its maximum value at the origin i.e. at $(\tau,\nu)=(0,0)$ and is always equal to $4E^2$.

$$\max\{\left|X(\tau,\nu)\right|^2\} = \left|X(0,0)\right|^2 = 4E^2 \tag{1.21}$$

$$\text{and,} \left|X(\tau,\nu)\right|^2 \le \left|X(0,0)\right|^2 \tag{1.22}$$

B. The ambiguity function is symmetric about the origin.

$$\left|X(\tau,\nu)\right| = \left|X(-\tau,-\nu)\right| \tag{1.23}$$

C. The ambiguity function has constant overall volume.

$$\iint \left|X(\tau,\nu)\right|^2 d\tau d\nu = (2E)^2 \tag{1.24}$$

D. For any signal $u(t)$ with a complex envelope has the ambiguity function $AF = \left|X(\tau,\nu)\right|$, the linear frequency modulation or quadratic phase modulation has the given response:

$$u(t) \Leftrightarrow \left|X(\tau,\nu)\right| \tag{1.25}$$

$$\Rightarrow u(t)\exp(j\pi kt^2) \Leftrightarrow \left|X(\tau,\nu-k\tau)\right| \tag{1.26}$$

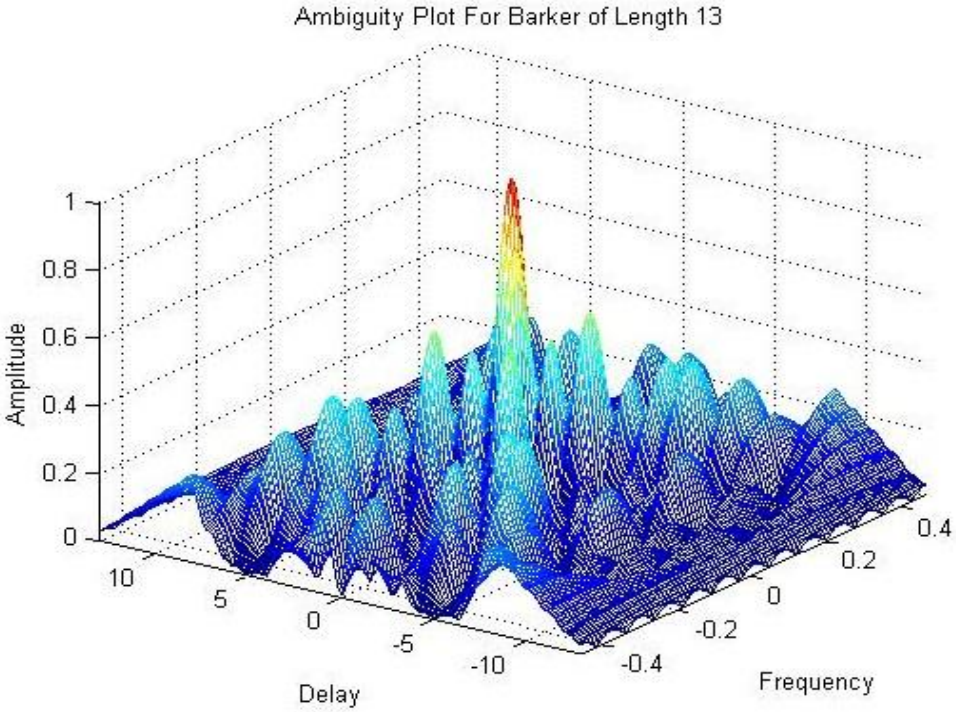

Figure 7. Plot for Barker coded signal ambiguity function

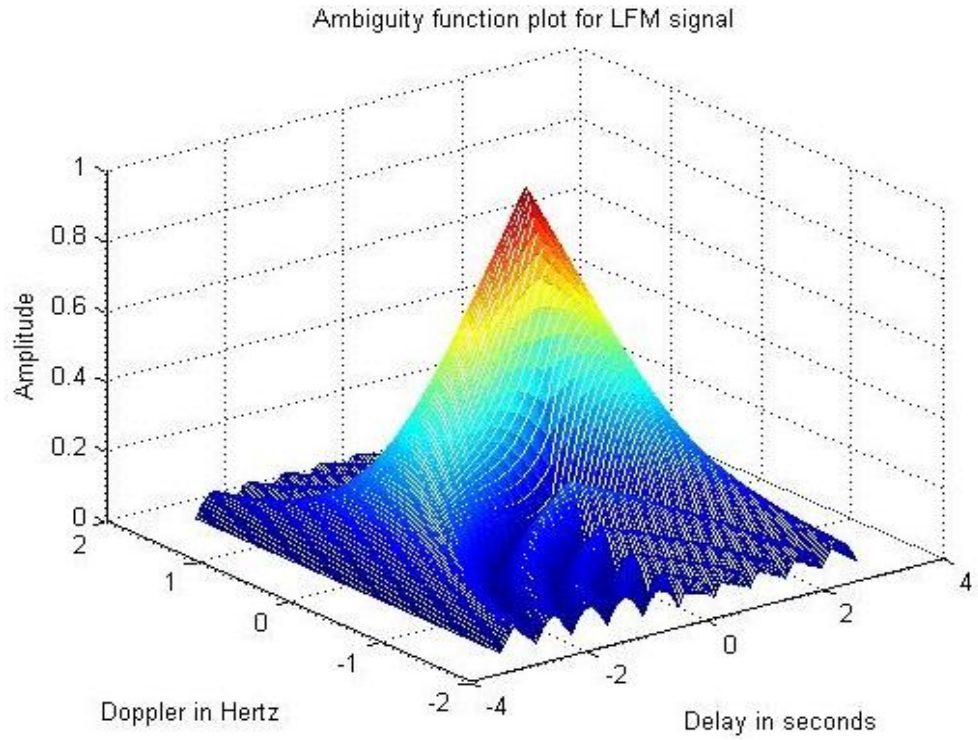

Figure 6. Plot for LFM signal ambiguity function

1.4 Radar Signals

A continuous signal with fixed frequency and a long time duration of T is not apt for radars as it is unable to resolve the range of the targets because of its narrow bandwidth, $B = \frac{1}{T}$.

Due to the above reason, modulation techniques in frequency or phase are implied which broadens the spectrum of the waveform and becomes capable of producing higher range resolution. Pulse compression methods are then implemented using the various mechanisms, where generally matched filter is used that compresses the signal into a duration of $\frac{1}{B}$.

1.4.1 Frequency Modulated Signals

Frequency modulation is the means for widening the spectrum of the pulse [2]. Linear Frequency Modulation(LFM) is the most famous method for achieving the frequency modulation of the pulse. In LFM, the instantaneous frequency of the signal varies linearly across the bandwidth B during the whole time duration T. Mathematically, the envelope of a normalized linear frequency modulated pulse is denoted by:

$$u(t) = \frac{1}{\sqrt{T}} rect\left(\frac{t}{T}\right) \exp\left(j\pi k t^2\right) \tag{1.27}$$

here, $k = \pm\frac{B}{T}$. k is the slope with which the frequency is changing through the whole time. '+' denotes the positive slope while '-' denotes the negative slope.

The phase at any instant of time is:

$$\phi(t) = \tfrac{1}{2}\left(kt^2\right) \tag{1.28}$$

Thus, the frequency at any instant of time can be easily found out by differentiating the instantaneous phase with respect to time.

$$f(t) = \frac{d}{dt}\phi(t) = kt \tag{1.29}$$

Thus, from the Eq. (1.28), it is clearly inferred that the frequency of the LFM is a linear function of time. Figure 10. depicts the matched filter response of the fixed frequency signal and the LFM signal.

The figure of merit for the pulse compression system is the measure of the peak sidelobe with respect to the mainlobe peak and the term used for this purpose is peak sidelobe ratio, given by:

$$PSLR = 10\log_{10}\frac{Peak\ Power\ of\ the\ Sidelobe}{Peak\ Power\ of\ the\ Mainlobe} \quad (1.30)$$

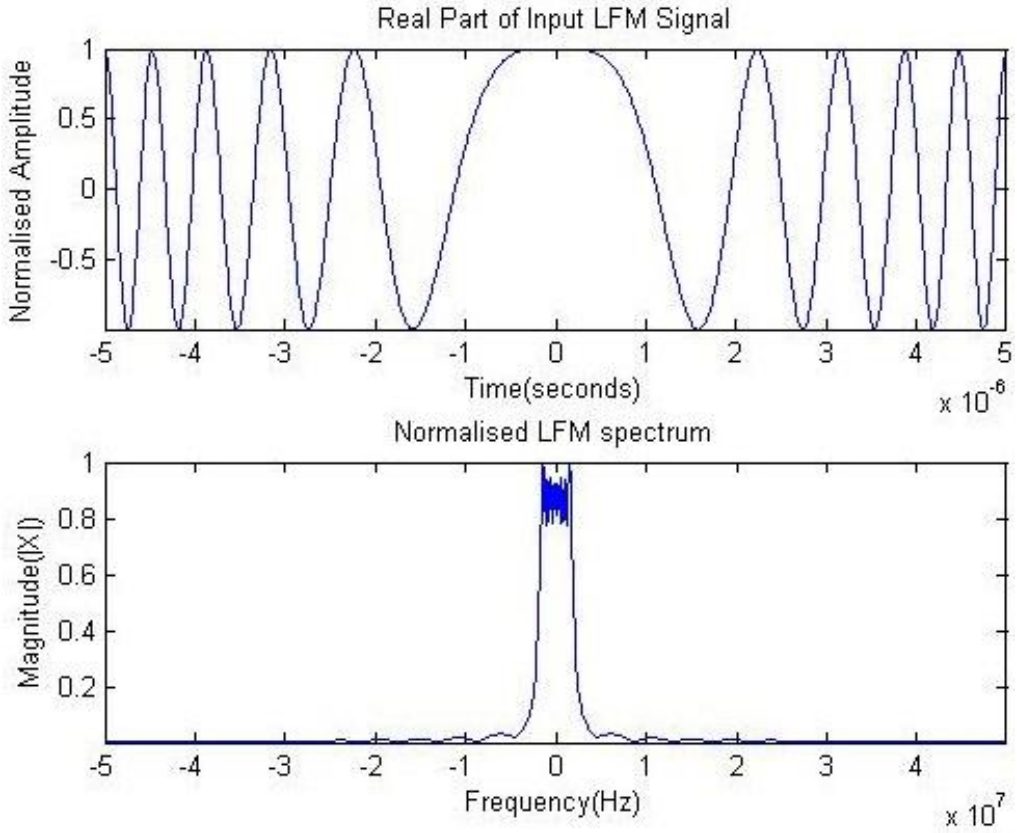

Figure 8. Plot for LFM component and its spectrum

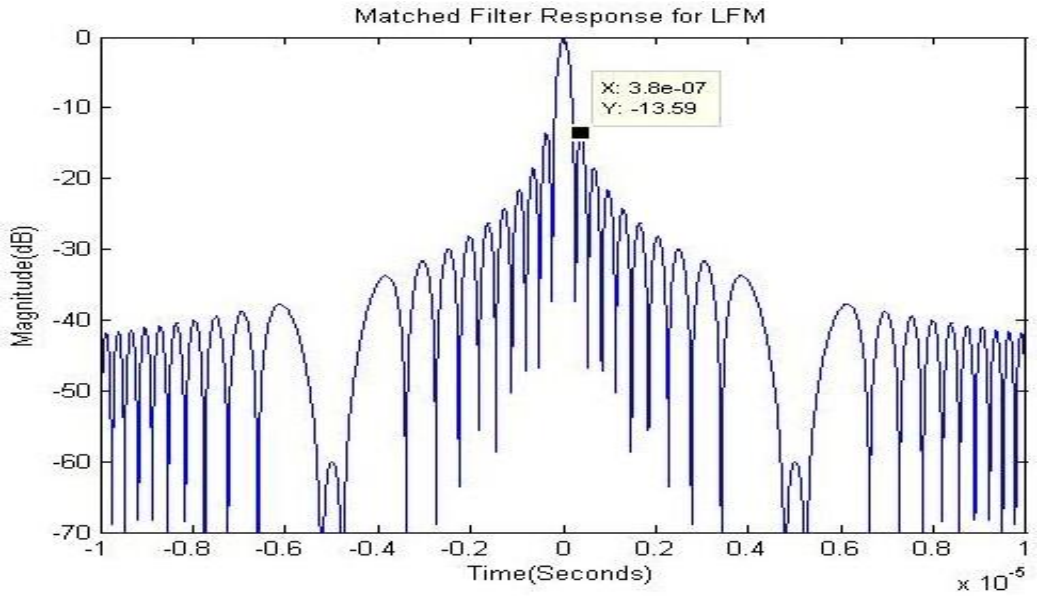

Figure 9. Plot for Autocorrelation Function of single LFM Pulse

The term PSLR is generally expressed in dB and hence the pulse compression systems are required to be designed in the same terms and expected to produce the least possible PSLR value. It can be clearly observed from Figure 10. that the output of the matched filter for the LFM pulse provides a quite high range resolution because of having a narrow mainlobe width. Beside the narrow mainlobe width, the output has also ambiguous sidelobes which hampers the detection of the weaker and nearby targets. For better detection lower sidelobes are favorable. The sidelobe with highest peak except the mainlobe peak are the peak sidelobes of the autocorrelation function.

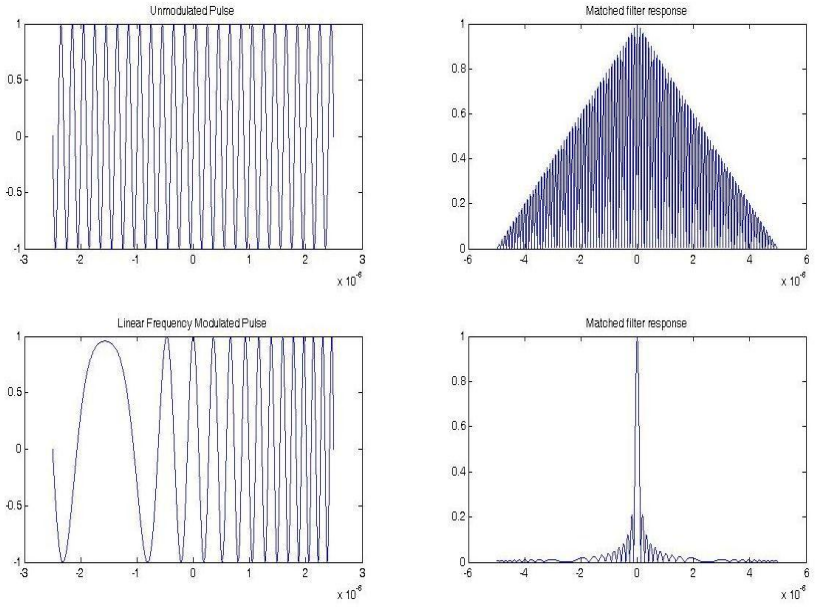

Figure 10. Autocorrelation Spectrum for unmodulated and linearly frequency modulated pulse

1.4.2 Pulse with Phase Modulation

As the phase coding pulse techniques are one of the initial methods employed for the compression in the radar signal processing. Here, a long time, T , duration pulse is divided into sub-pulses of equal duration, $t_b = T / N$, with N bits each, and each of the bits are then given a different phase value. The general complex envelope of any pulse with phase modulation is given by:

$$x(t) = \frac{1}{\sqrt{T}} \sum_{n=1}^{N} x_n rect\left[\frac{t-(n-1)t_b}{t_b} \right] \tag{1.31}$$

Where, $x_n = \exp(j\pi\varphi_n)$ and $\varphi_n = \{\varphi_1, \varphi_2, \varphi_3, ..., \varphi_N\}$ are phase codes for $x(t)$. Though there is a huge possible numbers of ways of generating a phase code but one most favorable ones are those which produce the optimal solution for the various conditions [2]. Desirable frequency spectrum, ease of implementation and the robustness in resolution properties of the pulse are the key points to select any phase code. In a most simple fashion, the binary phase shift keying technique shows the pulse compression by phase modulation, as in that

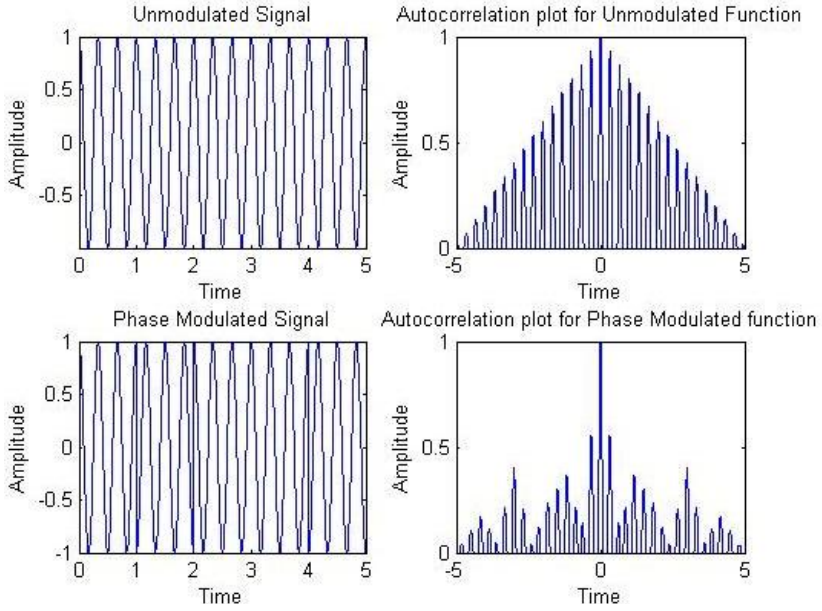

Figure 11. Autocorrelation spectrum for Unmodulated and Phase Modulated Signal

case the code constitutes of n bits that are either 0° i.e. in phase or 180° i.e. out of phase with the reference bit. Figure 11. depicts the output of a binary phase coded signal of length 5 bits when pulse compressed using a matched filter. The sequence taken here is [1 -1 1 1 -1].

1.5 Discussion

The process of pulse compression provides the radar designer with an ability to enhance the range resolution of the radar systems using a transmitter of low power by improving the overall bandwidth of the signal. It also reduces the bulkiness of the system but increases the complexity of the transceiver. Though LFM signal has a diverse role to play in the pulse compression, it also has few disadvantages. The LFM signal enhances the bandwidth of the transmitted signal resulting into betterment of the range resolution of the system. The range resolution is enhanced by a factor of the time-bandwidth product of the signal. The problem

with the LFM signal is that it has high sidelobe value which are potential of masking the small targets.

To overcome the high sidelobe level of the LFM signal few measures are there, like weighting in time domain and in frequency domain or the use of the NLFM signal. While using the amplitude modulation in time domain, the SNR of the transmitted signal goes low and hence the transmitted power is diminished which is undesirable. Also, if the weighting is done in the frequency domain the mainlobe width gets broadened which as a result decreases the range resolution but enhances the detection amplitude.

Chapter 2

Sidelobe suppression for Barker Code

2.1. Pulse Compression for Phase Coded Signals

Phase coded signals are formed by the division of a long duration pulse with a time duration of T into sub-pulses of N numbers where each sub-pulse has the width of τ. In the pulse compression of these signals the bandwidth of the signals is increased by varying the phase of the corresponding sub-pulse [2]. Each of the sub-pulse is having the phase of either 0 radian or π radians.

Here also, for the simple pulse compression, a matched filter is used. This matched filter produces the output of a spike with duration τ and an amplitude of N and the length of the output is the convolution length of the corresponding pulse. It has the compression ratio of $T/\tau \approx BT$, as $B \approx 1/\tau$ is the bandwidth of the signal. The waveform at the output of the matched has the length of N spanned to the either side of the peak or the central lobe. The lobes excluding the peak are called as the side-lobes of the output.

2.2. Barker codes

Generally, random choices are made for the binary states of 0 or π phases for each of the sub-pulse, constituting a barker code. Among those random choices, some of the random combinations are better than the others for a particular type of radar application. The primary goal while making such random combinations is that the autocorrelation of those phase coded pulses must have their side-lobes equal [12]. These codes are called barker codes only when they produce equalized side-lobes after being passed through the matched filter. For illustration, Figure 12. is used that shows a barker code of length 13 and Figure 13. shows its output of the matched filter when that signal is provided as the input to the matched filter. The auto-correlation output has six side-lobes of equal amplitude at the either side of the

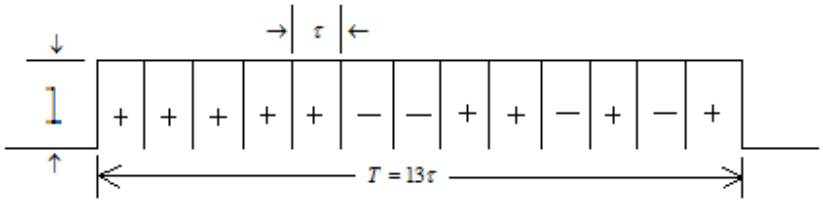

Figure 12. A Barker code with length 13

main-lobe that are 22.28 dB less than the main-lobe amplitude. The barker code with the length 13 is the longest one in its category.

The barker codes are binary phased code in which the codes have the phase value of 0 or π and its autocorrelation generates side-lobes of equal magnitude. X. Wu and J. S. Fu have given an adaptive filtering method that enhances the PCR and suppresses the side-lobes using LMS and RLS method [14]. The signal to sidelobe ratio (SSR) of the output is improved but it has low Doppler tolerance. A filter is proposed by B. Zrnic, A. Zezak and I. Simik that is based on the modified RLS algorithm using self-clutter suppression method shows better results compared to its counterpart i.e. the RLS algorithm [15].

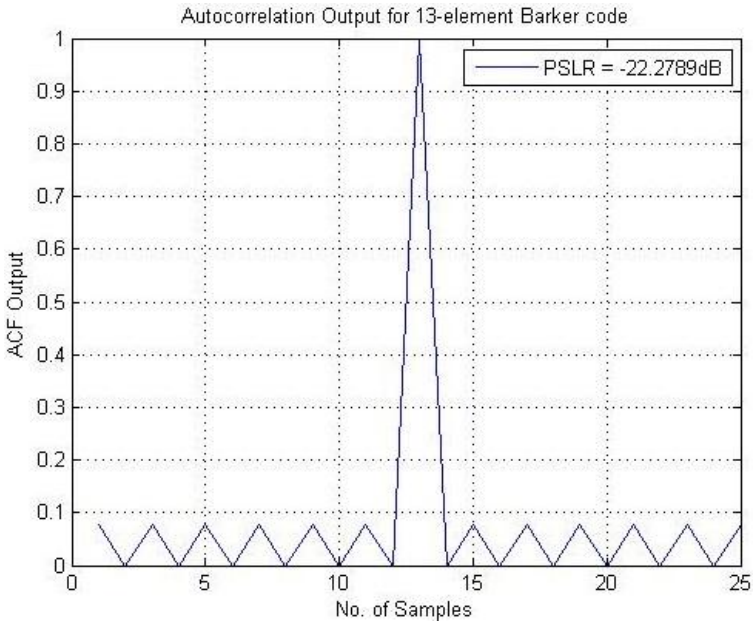

Figure 13. Output of the Matched Filter

2.3 Matched filter response of the Barker codes

As discussed in the previous chapter, the matched filter simply maximizes the peak signal to noise ratio (SNR) of the input signal at its output, which in turn helps in maximizing the detectability of the target by the radar system [13]. The system response of the matched filter is proportional the complex conjugate of the spectrum of signal at its input terminal. Mathematically, it is

$$H(f) = KS^*(f)exp(-j2\pi ft_m) \tag{2.1}$$

here, K is the proportionality constant, t_m is the time at which the matched filter produces maximum output, $S^*(f)$ is the conjugate of the complex envelope of the received pulse which acts as the input to the matched filter.

Also,

$$S(f) = \int_{-\infty}^{+\infty} s(t) exp(-j2\pi f t_m)\, dt \tag{2.2}$$

Thus the output of the matched filter is given as the cross-correlation of the replica of the transmitted waveform and the received pulse. While transmitting a rectangular pulse, the matched filter used is characterized by bandwidth, B , which is nearly reciprocal to the pulse width, τ , or can be approximated as $B\tau \approx 1$.

As a figure of merit, Peak to Side Lobe Ratio (PSLR) term is used which, mathematically, is given by:

$$PSLR = 10\log_{10} \frac{Peak\ power\ of\ the\ Side-lobe}{Peak\ power\ of\ the\ Main-lobe}$$

Table 2.1 Barker Code List with PSLR

Barker Code Length	Code phase	Peak To Side-lobe Ratio (dB)
2	+ -	- 6.00
3	+ + -	- 9.50
4	+ + - +	- 12.00
5	+ + + - +	- 14.00
7	+ + + - - + -	- 16.90
11	+ + + - - - + - - + -	- 20.80
13	+ + + + + - - + + - + -+	- 22.28

2.4 Adaptive Filter Implementation

Besides using a matched filter, an adaptive filter with N-tap can be used for better PSLR [14]. This can be done by taking barker code of length 13 as the input to the filter a desired output which produces a result only at the desirable instant of time. Also, the weights of the adaptive filter is trained by using the respective algorithm.

In the new age, adaptive filtering techniques are very powerful mechanism for signal processing applications as they have the ability of operating sufficiently good even in the unfamiliar conditions and trail the time variations of the input signal. They have been of

immense importance in various diversified fields such as biomedical engineering, radar and sonar applications, communication processes etc [17], [18]. The general architecture of an adaptive filtering procedure is shown below.

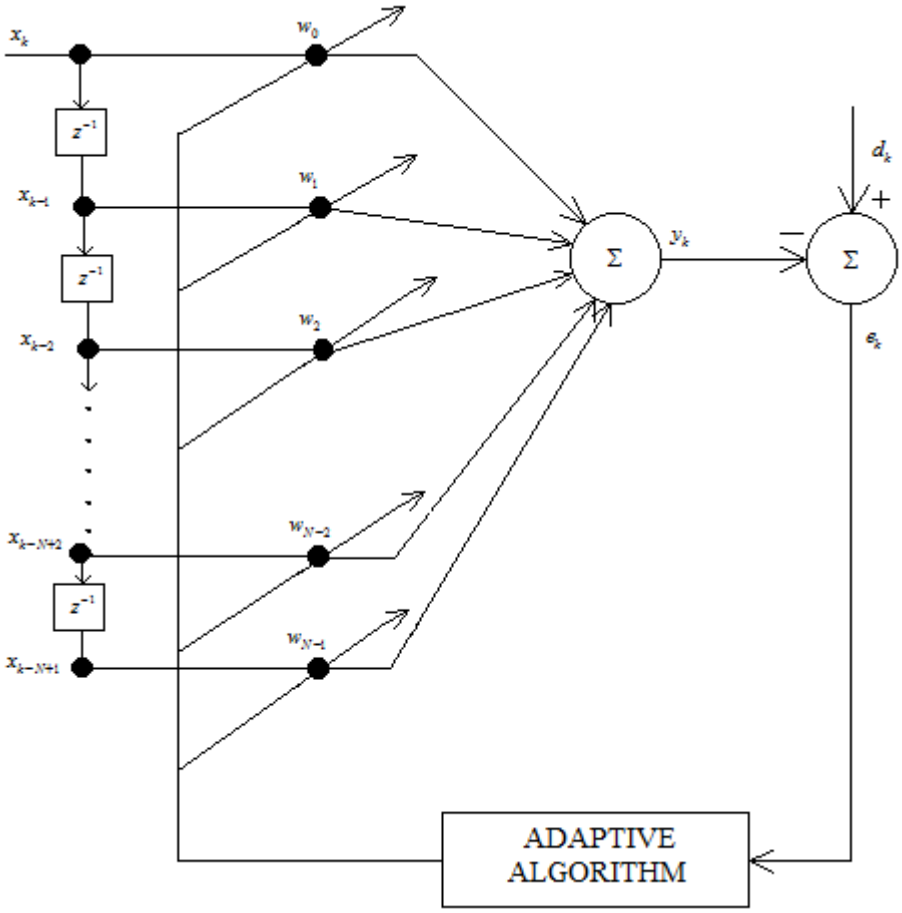

Figure 14. Adaptive Filtering Architecture

The above Figure 14. depicts an adaptive filter as a linear combiner. The adaptive filters have the input vector x_k and the desired response d_k are employed to calculate the error vector e_k which in turn manipulates the weights of the filter via the adaptive algorithms used. The filter coefficients are adjustable as per the requirement of the environmental conditions.

2.4.1 Least Mean Square (LMS) Algorithm

The least mean square algorithm is one of the most used adaptive filtering techniques in adaptive signal processing area. The ease of computation and the simplicity in implementation makes it one of the most favored algorithm as the repetition of data and gradient estimations for off-line cases are not required in this methodology [19]. Now, considering an arbitrary input vector provided to the filter be

$X_k = [x_k, x_{k-1}, x_{k-2}, ..., x_{k-N+2}, x_{k-N+1}]$ and initially the tap weight vector for the filter be $W_k = [w_0, w_1, w_2, ..., w_{N-2}, w_{N-1}]$.

The output y_k for the linear combiner architecture will be:

$$y_k = X_k^T W_k \tag{2.3}$$

The instantaneous error at any time k will be:

$$\begin{aligned} e_k &= d_k - y_k \\ &= d_k - X_k^T W_k \end{aligned} \tag{2.4}$$

here, d_k is desired response at any time index k.

While developing LMS algorithm, the square of the error vector, e_k^2, is considered for the estimation of the gradient. Thus, the estimation for the gradient vector in each of the iterations is found by:

$$\begin{aligned} \hat{\nabla}_k &= \begin{bmatrix} \frac{\partial e_k^2}{\partial w_0} \\ . \\ . \\ . \\ \frac{\partial e_k^2}{\partial w_{N-1}} \end{bmatrix} \\ &= 2e_k \begin{bmatrix} \frac{\partial e_k}{\partial w_0} \\ . \\ . \\ . \\ \frac{\partial e_k}{\partial w_{N-1}} \end{bmatrix} \\ &= -2e_k X_k \end{aligned} \tag{2.5}$$

The Eq. (2.5) calculates the derivative of the error vector with respect to the corresponding tap weights estimated in Eq. (2.4).

As the steepest descent algorithm expresses the iterative tap weight vector as:

$$W_{k+1} = W_k - \mu \hat{\nabla}_k \tag{2.6}$$

here μ is the step size regulating element called the gain constant.

Now, substituting the value of gradient, $\hat{\nabla}_k$, from Eq. (2.5) into Eq. (2.6), the tap weight update expression for LMS is found to be:

$$W_{k+1} = W_k + 2\mu e_k X_k \tag{2.7}$$

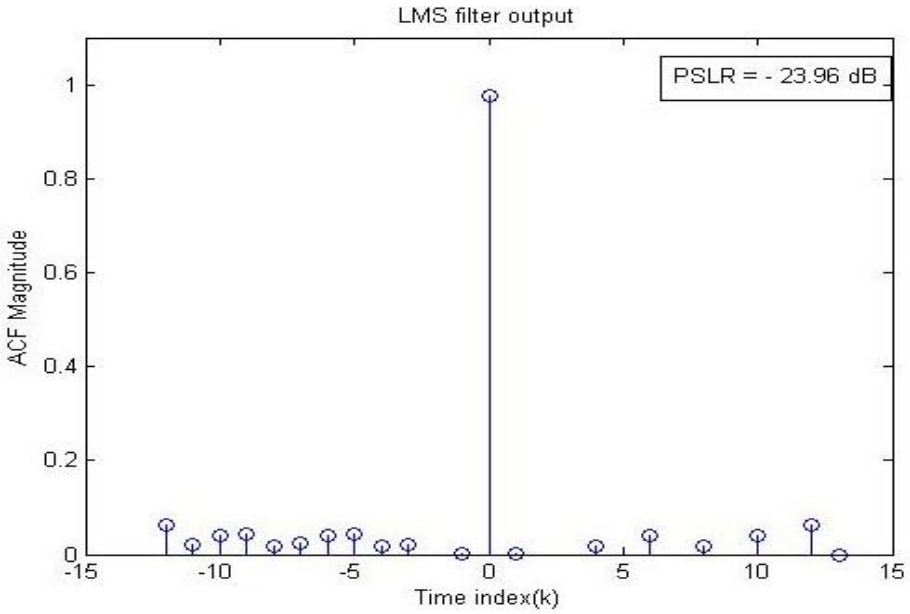

Figure 15. Plot showing LMS filter output

The dimension of the gain constant is reciprocal to the signal power. The process involves the weight update in each iterations till the error vector gets optimized and the gradient estimation is minimized.

2.4.2 Recursive Least Square(RLS) Algorithm

The development of the RLS algorithm was done on the basis of the matrix inversion lemma. Though the algorithm has the drawback of increase in the computational complexity, it provides a faster convergence rate with respect to its counterpart, the LMS algorithm. The convergence rate is however dominates the increase in the computational complexity, which in turn make the RLS algorithm more preferable [15], [16].

Considering $X_k = [x_k, x_{k-1}, x_{k-2}, ..., x_{k-N+2}, x_{k-N+1}]$ as the input vector, the initial tap weight vector of the filter as $W_k = [w_0, w_1, w_2, ..., w_{N-2}, w_{N-1}]$, d_k as the desired response of the filter and the assumption that the autocorrelation matrix R_k is having its inverse possible, the algorithm follows the following steps to reach the optimal solution [15], [20]:

A) $\{X_k, d_k\}$ are accepted as new samples.

B) X_k is formed by shifting its elements into information vector.

C) Priory output is calculated as:

$$y_0(k) = W_k^{0T} X(k) \tag{2.8}$$

D) Computing priory error as:

$$e_0(k) = d(k) - y_0(k) \tag{2.9}$$

E) Filtered information vector is computed as:

$$Z(k) = R_k^{-1} X(k) \tag{2.10}$$

F) Computing normalized error power as:

$$q = X^T(k) Z(k) \tag{2.11}$$

G) Gain constant is given by:

$$v = \frac{1}{1+q} \tag{2.12}$$

H) Normalized information vector is computed by:

$$\bar{Z}(k) = vZ(k) \tag{2.13}$$

I) Optimal filter tap weight vector is modified from W_k^0 to W_{k+1}^0 at each iteration by:

$$W_{k+1}^0 = W_k^0 + e_0(k)\bar{Z}(k) \tag{2.14}$$

J) The inverse correlation matrix is updated after every iteration as:

$$R_{k+1}^{-1} = R_k^{-1} - \bar{Z}(k)\bar{Z}^T(k) \tag{2.15}$$

Prior to start the iteration, the autocorrelation matrix R_k^{-1} is initiated as:

$$R_k^{-1} = \eta I_N \tag{2.16}$$

Here, I_N being the identity matrix of order $N \times N$ and η is the constant initialized with a large number such as 10^3 or 10^4.

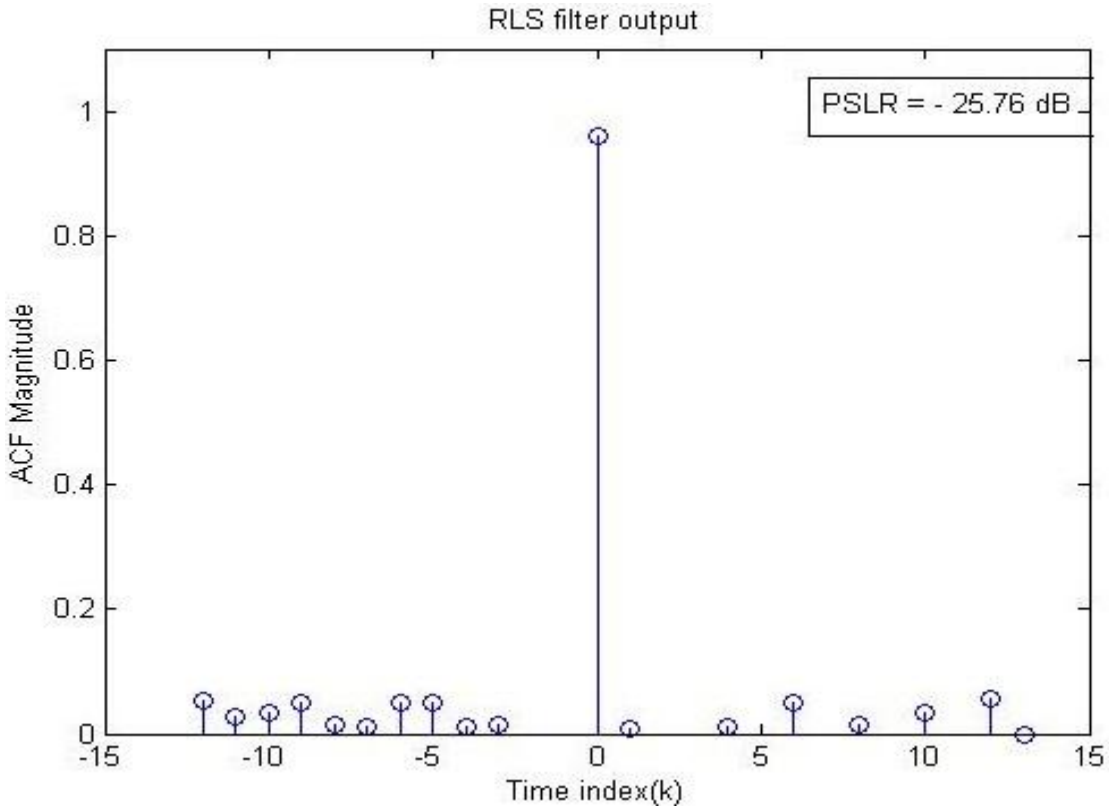

Figure 16. Plot showing RLS filter output

2.5 Simulated Results and Discussion

The matched filter is capable of performing pulse compression but is associated with sidelobes that are potential of masking the smaller targets and suffers with degradation in the noisy working conditions. The adaptive filters are better options to be used as they are robust while working in noisy conditions.

Table 2.2 Comparison of PSLR values for different filters

Filter Used	PSLR Obtained(dB)
1. Matched Filter	- 22.28
2. LMS Filter	- 23.96
3. RLS Filter	- 25.76

A filter of 13-tap is taken and trained in adaptive manner using the algorithms LMS and RLS. A shifted version of the barker codes are given as the input to the filter. The desired

signal output is modeled in a way that it has only mainlobe and the sidelobes be zero. The adaptive filter is trained in a way to minimize all the side lobes so that the ratio of the mainlobe peak to sidelobe gets minimized. The peak lobe power to sidelobe power is compared in the table below.

The table compares the PSLR obtained from matched filter, LMS filter and the RLS filter. It shows that the RLS filter outworks the matched and LMS filters.

Chapter 3

Sidelobe suppression in LFM pulse using windows

Traditional radars have the problem of optimizing the peak power requirement for the transmitted pulse and the range resolution of the same. Pulse compression technique has overcome that problem as it facilitates the combination of both features, peak power requirement and resolution, of the Radar. Simple pulse compression can be achieved by the use of the matched filter. But, the process has the demerit of high peak to sidelobe ratio (PSLR) of the observation spectrum of the received pulse. So various methods are used to subsidize the PSLR so that the detection can be proper and robust. This paper enquires about the application of the windows in maximizing the PSLR Matched filter's transfer function in frequency domain is the complex conjugate of the input signal's spectrum [1], [13]. It has the ability to concentrate the pulse energy. As the shorter pulse width signal has the higher range resolution but is quite inefficient towards attaining high range measurements due to low power content. So, pulse compression technique has overcome that problem as it facilitates the combination of both features, peak power requirement and resolution, of the Radar. But the matched filter compression suffers with the high PSLR that are potent of masking small targets. To maximize the PSLR, windowing is used [21], [24].

3.1 Window Functions

The sidelobes in the autocorrelation function of the transmitted pulse and the received pulse can be attenuated to a good extent by using the windowing functions. The windows are known to be mathematical functions that have pass band only to some selected range of time or frequency and outside that range the values are zero. There are many types of windows known. When a window function is multiplied with the other function, they gives zero value outside the pass band range which is the defined interval for window [23]. The windowing functions are also known as the weighting functions, which can be applied on any side of the processing unit *viz.* either on the transmitter side or the receiver side. But, the implementation of the weighting functions on the transmitter side results in the loss of the transmitted power and is beneficial to employ on the receiver side of the processing unit. Some of the window functions used in the simulation here are:

A) Hamming Window: This window minimizes the maximum side lobe in an optimized fashion. The mathematical expression of this type of window is:

$$w_{hamm}(n)=\begin{cases}0.54-0.46\cos\left(\dfrac{2\pi n}{N-1}\right), & \forall|n|\le\dfrac{N-1}{2}\\ 0, & \text{otherwise}\end{cases} \tag{3.1}$$

B) Hanning Window: These windows have zero value outside the pass band. Mathematically, it is given by:

$$w_{hann}(n)=\begin{cases}0.50-0.50\cos\left(\dfrac{2\pi n}{N-1}\right), & \forall|n|\le\dfrac{N-1}{2}\\ 0, & \text{otherwise}\end{cases} \tag{3.2}$$

C) Blackman Window: This window is expressed as:

$$w_{blackman}(n)=\begin{cases}0.42-0.50\cos\left(\dfrac{2\pi n}{N-1}\right)+0.0768\cos\left(\dfrac{4\pi n}{N-1}\right), & \forall|n|\le\dfrac{N-1}{2}\\ 0, & \text{otherwise}\end{cases} \tag{3.3}$$

D) Flattop Window: This window has partly negative value and in frequency domain it has flat top. They are quite helpful in measurement of amplitude of sinusoidal frequency components. It is given as:

$$w_{flattop}(n)=\begin{cases}1-1.93\cos\left(\dfrac{2\pi n}{N-1}\right)+1.29\cos\left(\dfrac{4\pi n}{N-1}\right)\\ \qquad -0.388\cos\left(\dfrac{6\pi n}{N-1}\right)+0.028\left(\dfrac{8\pi n}{N-1}\right), \forall|n|\le\dfrac{N-1}{2}\\ 0, \qquad \text{otherwise}\end{cases} \tag{3.4}$$

E) Bartlett Window: It is also known as the triangular window which can be formed by the convolution of two equal length rectangular window. It is expressed as:

$$w_{bartlett}(n)=\begin{cases}1-\left|\dfrac{n-\dfrac{N-1}{2}}{\dfrac{L}{2}}\right| & \forall|n|\le\dfrac{N-1}{2}\\ 0, & \text{otherwise}\end{cases} \tag{3.5}$$

3.2 Linear Frequency Modulated Pulse

LFM signals are generally used in RADARs because of their easy generation and have the compressed pulse shape that are insensitive to the Doppler shifts.

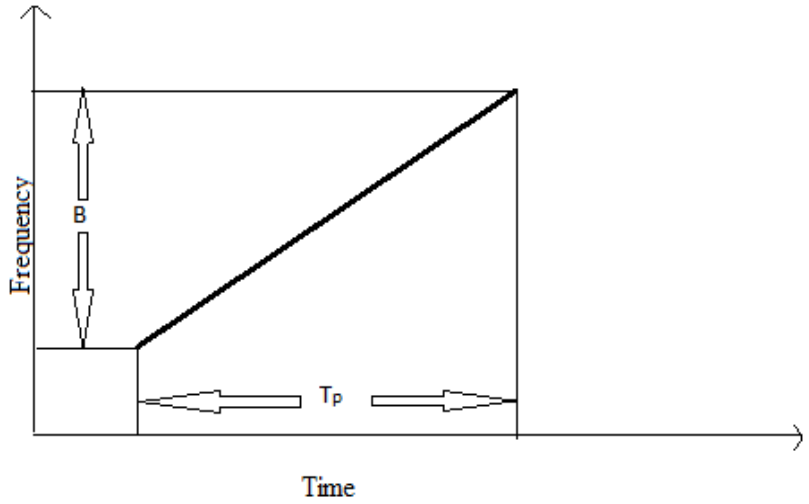

Figure 17. Plot for instantaneous Frequency v/s Time for LFM signal

LFM signal is denoted by:

$$e^{j\beta(t)} = \cos\beta(t) + j\sin\beta(t) \tag{3.6}$$

where, $\beta(t)$ is the instantaneous phase of the LFM pulse, given by:

$$\beta(t) = 2\pi\left(f_0 t \pm \frac{1}{2}kt^2 \right) \tag{3.7}$$

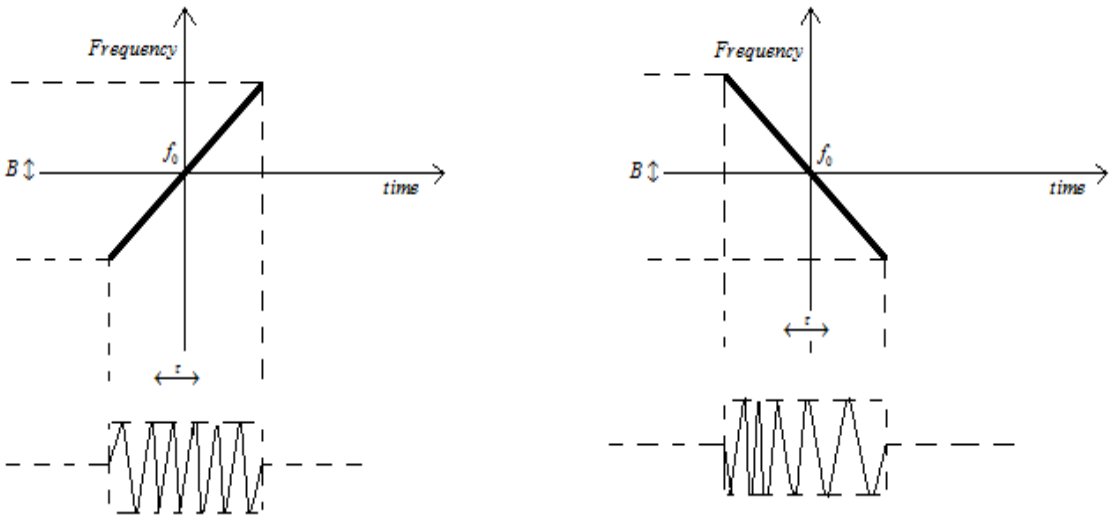

Figure 18. Plot showing positive and negative Frequency-Time slope of LFM pulse

3.3 Windowing of the LFM

Windows are applied through the weighting functions in the process of maximization of the PSLR. The basic building block of the process is as follows [25]:

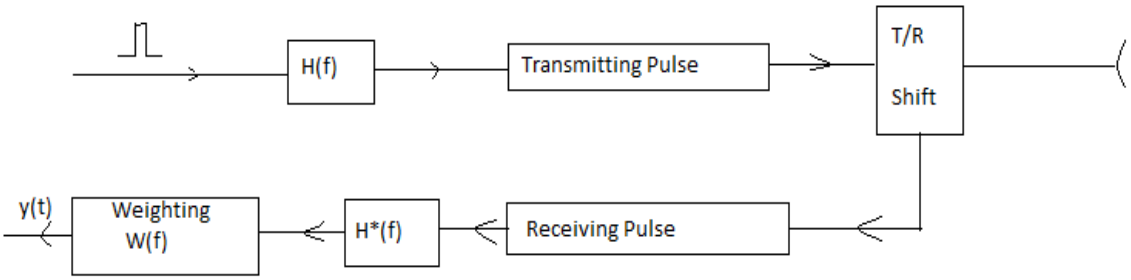

Figure 19. Block diagram depicting sidelobe suppression of LFM pulse

The FFT is the basic building block for sidelobe suppression while compressing the LFM pulse on the receiver side. While calculating the FFT of the pulse, it is assumed that the pulse is periodic. But, it is not the case that prevails always. For the signal being non-periodic, its frequency spectrum is affected with the leakage which further results into the smearing of the frequency components over a wide range and hence the frequency identification of the signal becomes tough. The windows are quite helpful in limiting the frequency range and thus also prohibits the leakages [22],[23]. Multiplying the window function with the non-periodic signal makes the signal periodic and also suppresses the sidelobes to a good extent. This can be done in both, time and frequency domain. Here it has been applied in time domain.

3.4 Simulation Results

For an LFM, the peak-to-sidelobe-ratio when compressed using the matched filter is -13.54 dB. The received signal, in time domain, is multiplied with the window function and then passed through the matched filter to get the output and the result is compared with the received signal passed through the matched filter without being multiplied with the window function. The PSLR is calculated using the Eq. (1.30).

The outputs of the different windowing operations are plotted and found that there is good improvement in the PSLR value of the compressed pulses but that is compensated by the widening of the main lobe width. As for the good range resolution, besides low side lobes, narrow mainlobe width is also required. Narrow main lobes are more efficient in detecting closely placed targets.

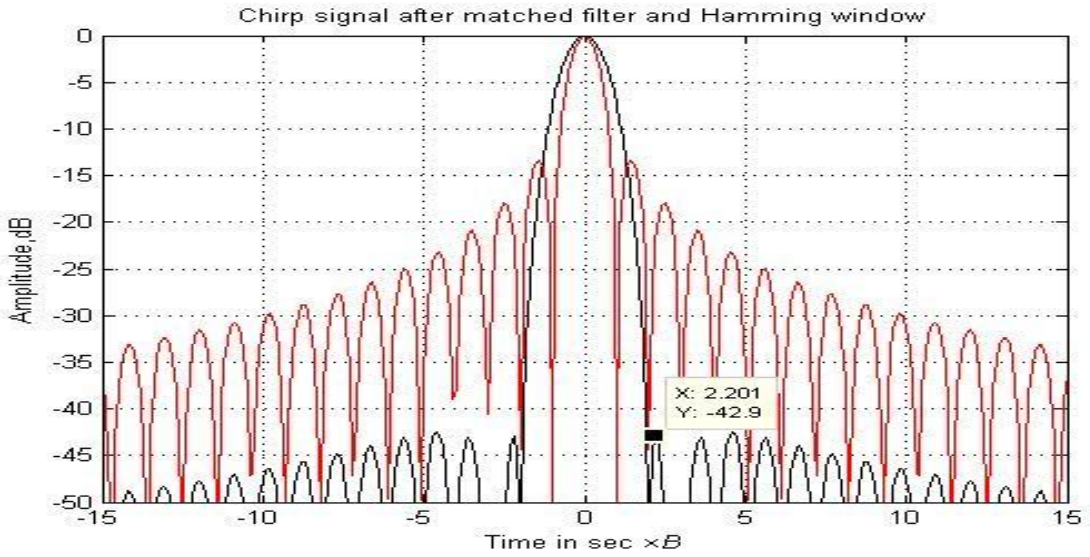

Figure 20. Sidelobe Suppression Using Hamming Window

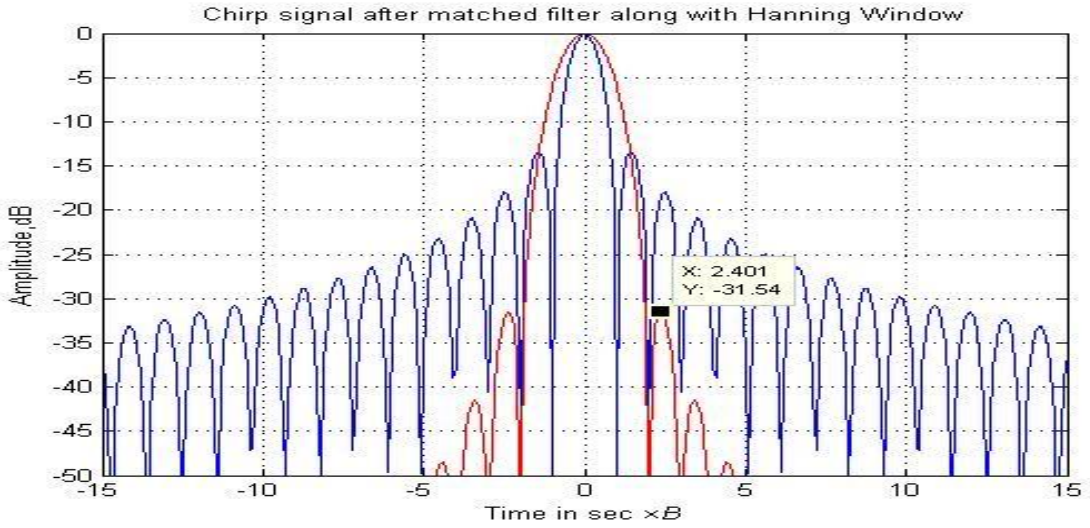

Figure 21. Sidelobe Suppression Using Hanning Window

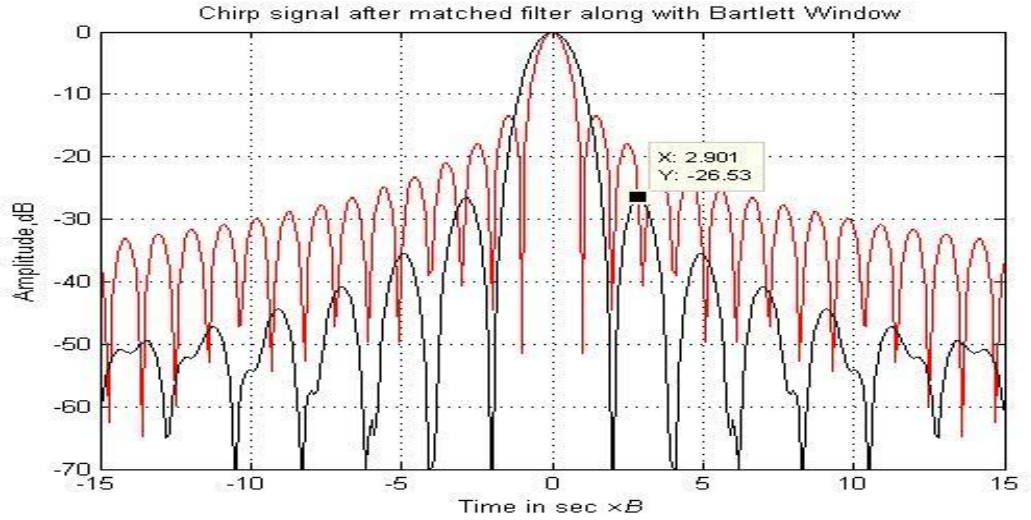

Figure 22. Sidelobe Suppression Using Bartlett Window

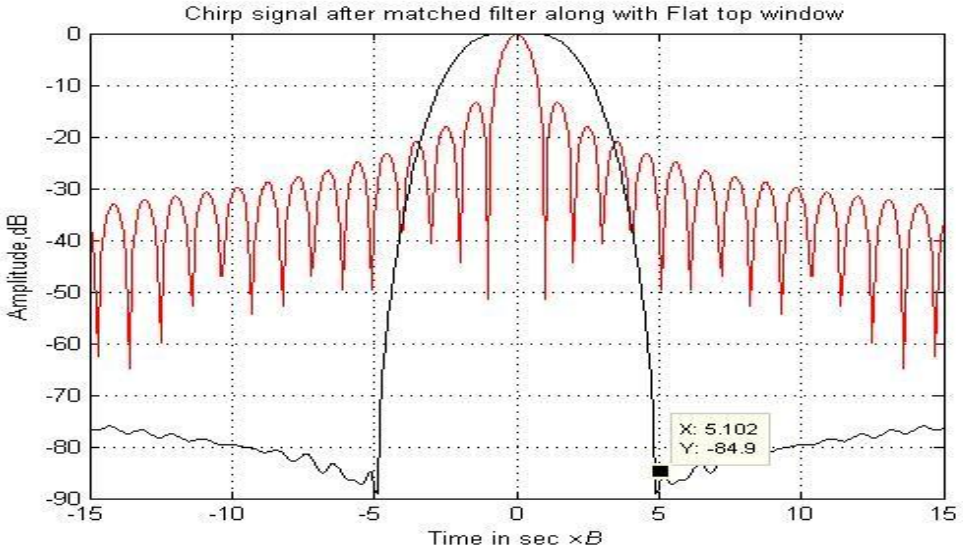

Figure 23. Sidelobe Suppression Using Flattop Window

Figure 20 and Figure 21 show the Hamming and Hanning widowed output, respectively. As both the window functions are raised cosine functions, they exhibits the similar frequency characteristics. But, the Hamming window has better suppression for initial sidelobes while the Hanning window gives better suppression for distantly placed sidelobes.

Figure 22, Figure 23 and Figure 24 show the outputs of Bartlett, Blackman and Flattop windows respectively. The width of the mainlobe of the Flattop windowed signal is highest among all but it also provides the maximum compression for the sidelobes. Because of its highest mainlobe width, the amplitude accuracy is maximum but has the poorest resolution.

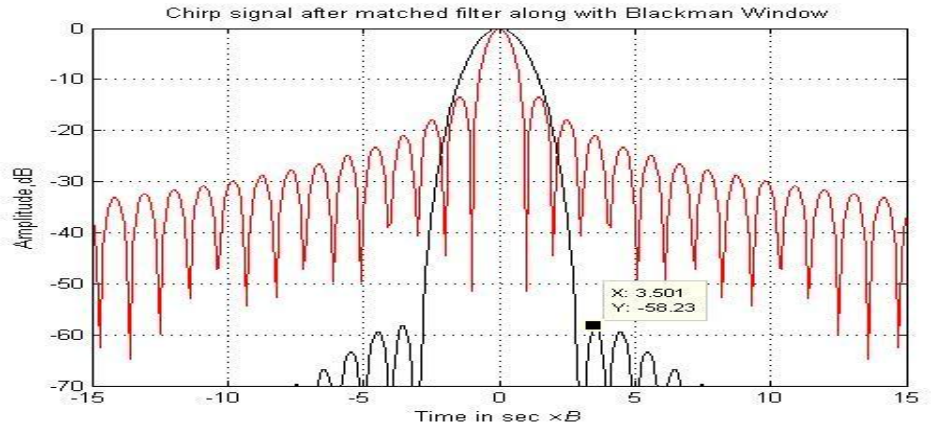

Figure 24. Sidelobe Suppression Using Blackman Window

Table 3.1 PSLR obtained for different Windows

Types of Window used	PSLR(dB)
Hamming	-42.90
Hanning	-31.54
Bartlett	-26.53
Blackman	-58.23
Flattop	-84.90

Though the windows are providing suppressed sidelobes, they have the common demerit of increase in mainlobe width. But, they are used in different applications as per the requirement. Lowest maximum sidelobe level windows are required in strongly interfering signals in the vicinity of the frequency of interest. For narrow placed targets, the widow with lowest possible mainlobe width is required. If the high accuracy in the measurement of

amplitude is needed then the window with highest mainlobe width is required. Because of the higher mainlobe width of the flattop window, its resolution is lowest and it is also tough for this window to determine the exact frequency components of the received signal. The Bartlett window shows better resolution because of narrow bandwidth and hence is capable of detecting the closely spaced target signals.

The results shows the suppression of the sidelobes is possible by using the window function for weighting the received signals. For an LFM pulse without the use of the window function, the PSLR value is -13.54dB, which is enhanced to different higher values with the use of the different window function. But, before choosing the window for a purpose it is necessary to look into its various related attributes like mainlobe width, compressed pulse width, PSLR provided etc. so as to use them more effectively.

Chapter 4
Suppression of grating lobes in stepped frequency train of LFM pulse

4.1 Stepped frequency train of LFM pulse

The range resolution of the linear frequency modulated radar signal can be enhanced by employing stepping of frequency between two consecutive transmitted pulses. By doing so, the total bandwidth of the signal is increased. This is done by using coherent train of stepped frequency pulses. In this method, the overall bandwidth of the signal gets enhanced while the transmitted pulses have a low instantaneous bandwidth. Moreover, the duration between the stepped pulses can be efficiently used by the radar system to accommodate the narrow frequency change between the consecutive pulses. If the stepping frequency is large then a large overall bandwidth is achieved [27], [28].

But this approach of achieving a large overall bandwidth is associated with the occurrence of the ambiguous peaks, also known as the 'grating lobes', when the product of the stepped frequency and the pulse duration becomes greater than unity. It is also noticed that the grating lobes can be reduced by using the LFM pulses instead of continuous frequency signals. The LFM pulses are stepped with frequency Δf to reduce the effect of those grating lobes. The ACF of the train of pulses have the grating lobes while the ACF of the single LFM pulse has side lobes and nulls [31].

4.2 AF for stepped frequency train of LFM pulses

As the range resolution and the signal bandwidth are inversely related for a radar system, the stepped frequency train of LFM signal is an efficient procedure to enhance the total bandwidth of the transmitted pulse. Besides the procedure provides the system to adjust the center frequency between the consecutive pulses, it also produces grating lobes along with the mainlobe [30].

An LFM has a complex envelope denoted as [31]:

$$u(t) = \frac{1}{\sqrt{T_p}} rect\left(\frac{t}{T_p}\right) \exp\left(j\pi k t^2\right) \tag{4.1}$$

The LFM denoted by Eq. (4.1) has the unit energy as it is multiplied by the term $\frac{1}{\sqrt{T_p}}$, and k is the frequency slope present in the pulse given by:

$$k = \pm \frac{B}{T_p} \tag{4.2}$$

'+' and '-' signs represent the positive and negative frequency slope of the LFM pulse respectively. The AF of a single pulse LFM is given by:

$$\left|X(\tau,\nu)\right| = \left|\left(1-\frac{|\tau|}{T_p}\right)\mathrm{sinc}\left[T_p(\nu+k\tau)\left(1-\frac{|\tau|}{T_p}\right)\right]\right|, \qquad |\tau| \le T_p \tag{4.3}$$

Thus, a uniform train of the N number of such LFM pulses with unit energy can be written as:

$$u_N(t) = \frac{1}{\sqrt{N}}\sum_{n=0}^{N-1} u(t-nt_r) \tag{4.4}$$

Each of the LFM pulse is supposed to be separated by the duration t_r, which is the pulse repeating time and is always greater than the twice of the pulse duration i.e. $t_r \ge 2T_p$.

Now, for any delay τ less than the pulse duration T_p, the AF of the single pulse and the train of coherent pulses are related as:

$$\left|X_N(\tau,\nu)\right| = \left|X(\tau,\nu)\right|\left|\frac{\sin(N\pi\nu t_r)}{N\sin(\pi\nu t_r)}\right|, \qquad |\tau| \le T_p \tag{4.5}$$

Now, adding LFM to the whole train of pulses with different frequency slopes k_s, it becomes:

$$\begin{aligned} u_{train}(t) &= u_N(t)\exp\left(j\pi k_s t^2\right) \\ &= \frac{1}{\sqrt{N}}\exp\left(j\pi k_s t^2\right)\sum_{n=0}^{N-1} u(t-nt_r) \end{aligned} \tag{4.6}$$

where, $k_s = \pm\frac{\Delta f}{t_r}$, $\Delta f > 0$, is the frequency step which can be either positive or negative depending on the sign '+' or '-' respectively.

Again, according to the LFM property of the AF as discussed in Eq. (1.26) of Section 1.3.1, the addition of the LFM pulse will modify the AF of the train signal as:

$$\left|X_{train}(\tau,\nu)\right| = \left|X(\tau,\nu+k_s\tau)\right|\left|\frac{\sin(N\pi(\nu+k_s\tau)t_r)}{N\sin(\pi(\nu+k_s\tau)t_r)}\right|, \qquad |\tau| \le T_p \tag{4.7}$$

Now, using Eq. (4.3) in Eq. (4.7), we get

$$\left|X_{train}(\tau,\nu)\right| = \left|\left(1-\frac{|\tau|}{T_p}\right)\text{sinc}\left[T_p\left(\nu+\left(k+k_s\right)\tau\right)\left(1-\frac{|\tau|}{T_p}\right)\right]\right| \times \left|\frac{\sin\left(N\pi\left(\nu+k_s\tau\right)t_r\right)}{N\sin\left(\pi\left(\nu+k_s\tau\right)t_r\right)}\right|, \quad |\tau| \le T_p \tag{4.8}$$

Here, the slope k_s is added to get the frequency step which adds up to the original slope k of the single LFM pulse making the overall bandwidth as [29]:

$$B = \left|k+k_s\right|T_p \tag{4.9}$$

So, using the Eq. (4.9) in Eq. (4.8), we will get the AF of the stepped frequency train of LFM pulses as:

$$\left|X_{train}(\tau,\nu)\right| = \left|\left(1-\frac{|\tau|}{T_p}\right)\text{sinc}\left[T_p\left(\nu+B\frac{\tau}{T_p}\right)\left(1-\frac{|\tau|}{T_p}\right)\right]\right| \times \left|\frac{\sin\left(N\pi\left(\nu+\Delta f\frac{\tau}{t_r}\right)t_r\right)}{N\sin\left(\pi\left(\nu+\Delta f\frac{\tau}{t_r}\right)t_r\right)}\right|, \quad |\tau| \le T_p \tag{4.10}$$

4.3 Nullifying Condition for Grating lobes

To nullify the grating lobes, it is assumed that there is a zero Doppler shift in the received pulse. So, applying zero Doppler cut i.e. putting $\nu = 0$ into Eq. (4.10), which is ACF expression of the train of LFM pulses, yields [29], [30], [31]:

$$\left|R(\tau)\right| = \left|\left(1-\frac{|\tau|}{T_p}\right)\text{sinc}\left[B\tau\left(1-\frac{|\tau|}{T_p}\right)\right]\right|\left|\frac{\sin\left(N\pi\tau\Delta f\right)}{N\sin\left(\pi\tau\Delta f\right)}\right|, \quad |\tau| \le T_p \tag{4.11}$$

Eq. (4.11) can be seen as a product of two components - (a) The first component is because of an increased slope single LFM pulse:

$$\left|R_1(\tau)\right| = \left|\left(1-\frac{|\tau|}{T_p}\right)\text{sinc}\left[B\tau\left(1-\frac{|\tau|}{T_p}\right)\right]\right|, \quad |\tau| \le T_p \tag{4.12}$$

and (b) The second component gives rise to the grating lobes:

$$\left|R_2(\tau)\right| = \left|\frac{\sin\left(N\pi\tau\Delta f\right)}{N\sin\left(\pi\tau\Delta f\right)}\right|, \quad |\tau| \le T_p \tag{4.13}$$

$$= \left| \frac{\sin(N\pi\tau\Delta f)}{N\pi\tau\Delta f \dfrac{\sin(\pi\tau\Delta f)}{\pi\tau\Delta f}} \right|$$

$$= \left| \frac{\mathrm{sinc}(N\tau\Delta f)}{\mathrm{sinc}(\tau\Delta f)} \right|, \qquad |\tau| \le T_p \tag{4.14}$$

By Eq. (4.14), as $|R_2(\tau)|$ is the ratio of two *sinc* functions, it produces peak at the instants when $\mathrm{sinc}(\tau\Delta f)$ has a null or zero value [31] i.e. when

$$\begin{aligned} &\pi\tau\Delta f = n\pi \\ &\Rightarrow \tau\Delta f = n, \quad \text{where } n = 0, \pm1, \pm2, ..., \lfloor T_p\Delta f \rfloor \end{aligned} \tag{4.15}$$

or, $\tau_{lobes} = \dfrac{n}{\Delta f}$ (4.16)

As of now, the overall AF of the train of LFM pulse has two components, the grating lobes produced by $|R_2(\tau)|$ can be nullified if the nulls of $|R_1(\tau)|$ coincide with them. For doing so, the first two grating lobes and nulls are coincided while in some cases it nullifies all the grating lobes. If a fixed frequency pulse is used then the grating lobes are more prominent and they can't be nullified [31], which is depicted in Figure 25.

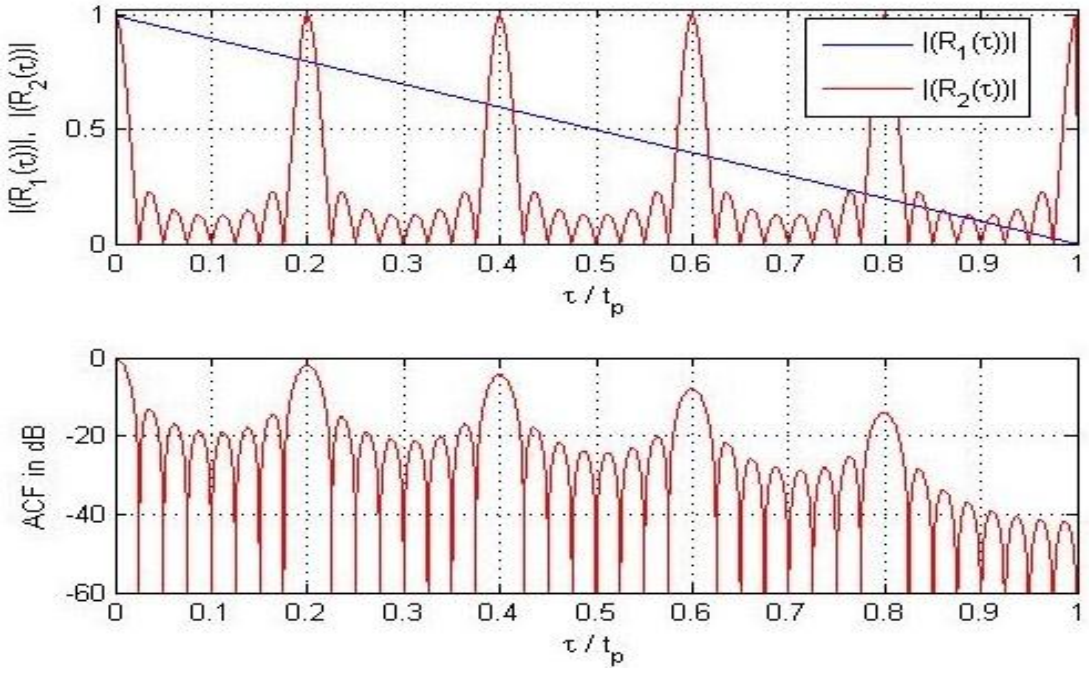

Figure 25. Top: AF for stepped frequency train of fixed frequency and Bottom: Partial ACF(in dB).(N=8, TpΔf=5, TpB=0)

4.4 $T_p\Delta f$ - T_pB relationship for grating lobe nullification

The generalized relation between $T_p\Delta f$ and T_pB is found in two parts [30]:

A. Case I – $T_p\Delta f \le 3$: When the number of grating lobes is not more than three. In such case, there is a symmetry about $\tau = \frac{T_p}{2}$ in the *sine* argument of Eq. (4.12) i.e. $\pi B\tau\left(1-\frac{|\tau|}{T_p}\right)$. The position of the first grating lobe can be found by the relation:

$$\pi B\tau\left(1-\frac{|\tau|}{T_p}\right)=\pi \tag{4.17}$$

$$\Rightarrow \frac{B}{\Delta f}\left(1-\frac{1}{T_p\Delta f}\right)=1 \tag{4.18}$$

$$\Rightarrow T_pB=\frac{\left(T_p\Delta f\right)^2}{T_p\Delta f-1} \tag{4.19}$$

Now, for $1<T_p\Delta f\le 2$, the first grating lobe is present in the second half of the pulse duration. So, for the situation, $1<T_p\Delta f\le 2 \Rightarrow 1\ge T_p\Delta f\ge \frac{1}{2}\Rightarrow T_p\ge \frac{1}{\Delta f}\ge \frac{T_p}{2}$ and finally $\frac{T_p}{2}\le\tau\le T_p$, which implies that if a null is placed on it then it will also place a null in the first half of the spectrum where there is no grating lobe. Thus, matching the first grating lobe is not possible in this case but to match a null at any location of the single grating lobe is possible.

Similarly, for specific values $T_p\Delta f=2$ and $T_pB=4$, the nulls at first two consecutive position coincide with each other at $\frac{T_p}{2}$ making the first grating lobe to match at the same position while the third null at T_p matches with the second grating lobe.

Again, when $2 < T_p\Delta f \le 3$, there will be a pair of symmetric nulls in both half of the pulse duration and the condition: $T_p B = \dfrac{\left(T_p\Delta f\right)^2}{2\left(T_p\Delta f - 2\right)}$, must hold true so that the second null and the second grating lobe matches.

B. Case II - $T_p\Delta f > 3$: in this case the number of grating lobes appear is more than or equal to three. Considering the m^{th} and n^{th} nulls of $\left|R_1(\tau)\right|$, where $n > m$, are exactly at q^{th} and r^{th}, where $r > q$, grating lobes of $\left|R_2(\tau)\right|$. So using the generalized cases of n, m, q and r, $\left|R_1(\tau)\right|$ and $\left|R_2(\tau)\right|$ will give the relations:

$$\pi B\frac{q}{\Delta f}\left(1-\frac{q}{T_p\Delta f}\right) = m\pi \tag{4.20}$$

$$\pi B\frac{r}{\Delta f}\left(1-\frac{r}{T_p\Delta f}\right) = n\pi \tag{4.21}$$

Equating the above Eq. (4.20) and Eq. (4.21) simultaneously,

$$\frac{q}{m}\left(1-\frac{q}{T_p\Delta f}\right) = \frac{r}{m}\left(1-\frac{r}{T_p\Delta f}\right)$$

$$\Rightarrow T_p\Delta f = \frac{mr^2 - nq^2}{mr - nq} \tag{4.22}$$

Thus for nullifying the first two grating lobes i.e.

$$T_p\Delta f = \left(\frac{mr^2 - nq^2}{mr - nq}\right)_{q=1,r=2} = \frac{4m-n}{2m-n} \tag{4.23}$$

Now, as $n \ge m$, $r > q$ and are all positive. Also, $\lfloor T_p\Delta f \rfloor$ shows the number of the grating lobes produced, it must be positive and greater than r.

The time bandwidth product, TBWP, for a valid $T_p\Delta f$ is:

$$\begin{aligned} T_p B &= \frac{n}{r\left(T_p \Delta f - r\right)}\left(T_p \Delta f\right)^2 \\ &= \frac{\left(mr^2 - nq^2\right)^2}{qr\left(r-q\right)\left(mr-nq\right)} \end{aligned} \tag{4.24}$$

And, like as above, for the first two grating lobes $T_p B$ becomes:

$$\begin{aligned} T_p B &= \left(\frac{\left(mr^2 - nq^2\right)^2}{qr\left(r-q\right)\left(mr-nq\right)} \right)_{q=1,r=2} \\ &= \frac{\left(4m-n\right)^2}{2\left(2m-n\right)} \end{aligned} \tag{4.25}$$

Now, the overlap ratio $\frac{B}{\Delta f}$ will be equal to:

$$\begin{aligned} \frac{B}{\Delta f} &= \frac{nT_p \Delta f}{r\left(T_p \Delta f - r\right)} \\ &= \frac{\left(mr^2 - nq^2\right)}{qr\left(r-q\right)} \end{aligned} \tag{4.26}$$

For the first two lobes, the overlap ratio becomes:

$$\begin{aligned} \frac{B}{\Delta f} &= \left(\frac{\left(mr^2 - nq^2\right)}{qr\left(r-q\right)} \right)_{q=1,r=2} \\ &= \left(\frac{4m-n}{2} \right) \end{aligned} \tag{4.27}$$

The overlap ratio must be less than the total number of pulses in order to achieve a significant raise in the bandwidth.

As of now, the parameters $T_p B$, $T_p \Delta f$ and $\frac{B}{\Delta f}$ are denoted in terms of *m*, *n*, *r* and *q*, the ACF can be written in terms of $T_p B$ and $T_p \Delta f$ as:

$$\left|R\left(\frac{\tau}{T_p}\right)\right| = \left|\left(1-\frac{|\tau|}{T_p}\right)\mathrm{sinc}\left[T_pB\frac{\tau}{T_p}\left(1-\frac{|\tau|}{T_p}\right)\right]\right| \times \left|\frac{\sin\left(N\pi T_p\Delta f\,\frac{\tau}{T_p}\right)}{N\sin\left(\pi T_p\Delta f\,\frac{\tau}{T_p}\right)}\right|, \qquad \left|\frac{\tau}{T_p}\right| \le 1 \tag{2.28}$$

4.5 Simulation results and discussions

Table 4.1 presents some of the possible valid values of the parameters *m, n, r* and *q* that shows the nullification of the grating lobes in the assumed case. For all the simulations, the number of pulses taken is 8 i.e. *N=8.*

Table 4.3 Few valid values for nullification of first two grating lobes

m	n	r	q	$T_p\Delta f$	T_pB	$\frac{B}{\Delta f}$
1	1	2	1	3	4.5	1.5
2	3	2	1	5	12.5	2.5
3	4	2	1	4	16	4
4	7	2	1	9	40.5	4.5

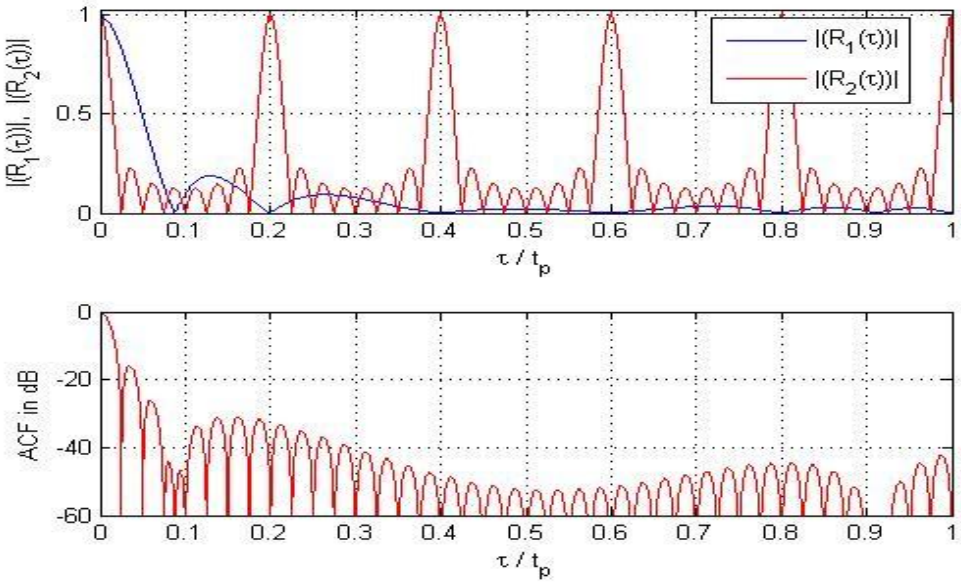

Figure 26. Plots showing suppression of grating lobes in SFT of LFM pulses with N=8, TpΔf=5, TpB=12.5(above)

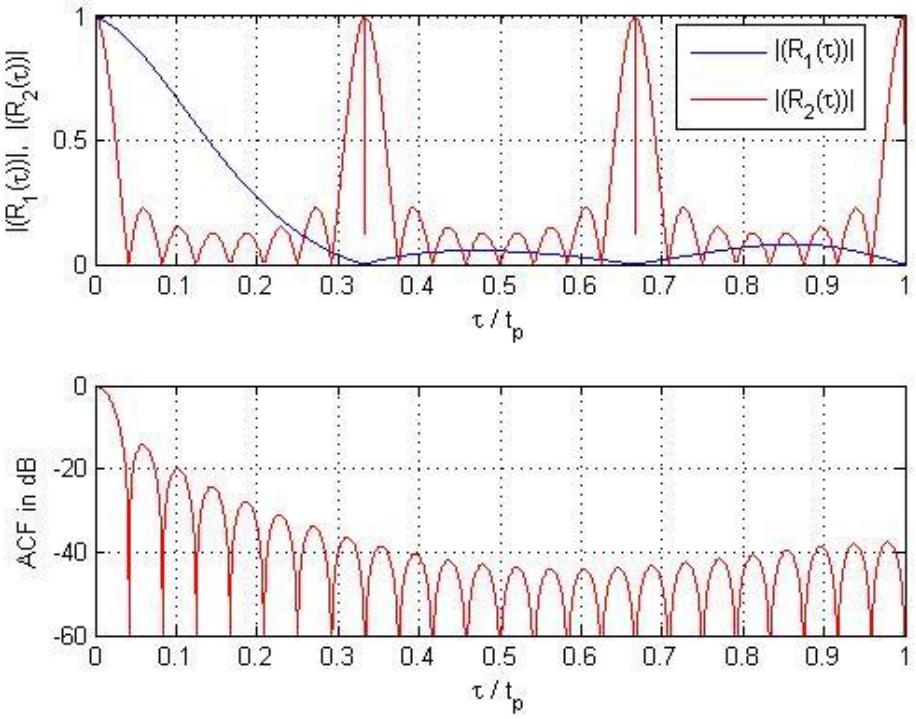

Figure 28. Plots showing suppression of grating lobes in SFT of LFM pulses with N=8, TpΔf=3, TpB=4.5(above) and Partial ACF in dB

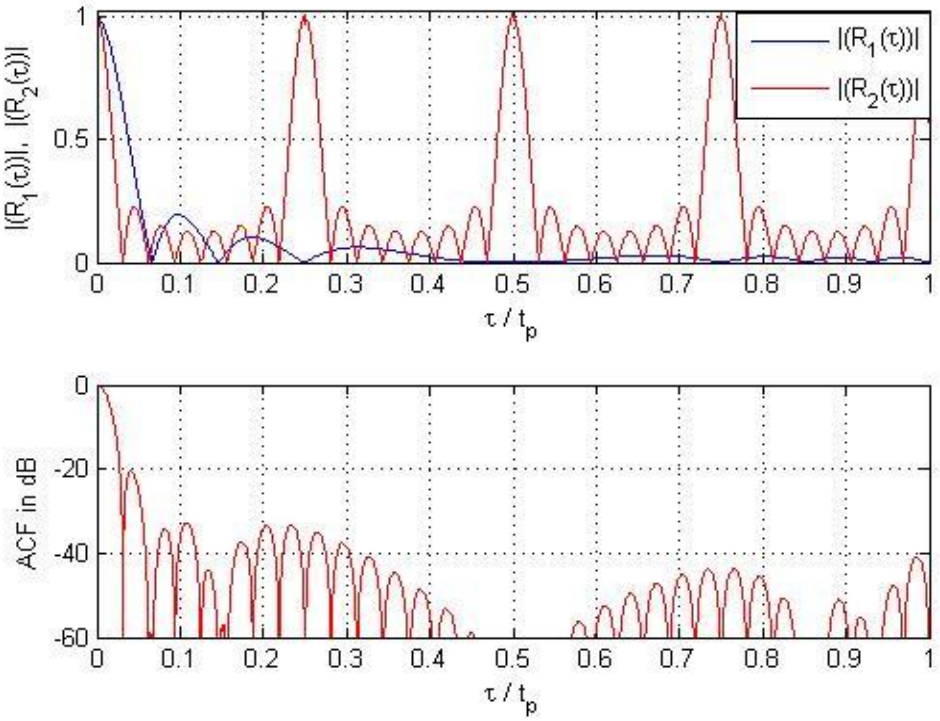

Figure 27. Plots showing suppression of grating lobes in SFT of LFM pulses N=8, TpΔf=4, TpB=16(above) and Partial ACF in dB (below)

Simulation plots verify the fact that the nulls of $\left|R_1(\tau)\right|$ are at the symmetrical location around the point $\tau = \frac{T_p}{2}$ and their number is the smallest integer value greater than $\frac{T_pB}{2}$ i.e. $\left\lceil \frac{T_pB}{2} \right\rceil$. The number of the peaks appear in the plot of $\left|R_2(\tau)\right|$ is equal to $\lfloor T_p\Delta f \rfloor$. Table 4.1 shows only four possible combinations of the values *n*, *m*, *r*, *q*, $T_p\Delta f$, T_pB and $\frac{T_p}{\Delta f}$, though a lot more combinations are possible.

Thus the overall bandwidth of the signal can be increased by employing the stepped frequency process to the train of LFM pulses which improves the range resolution of the signal. Though the constructed signal suffers with the grating lobe but that can be nullified by using proper values of the parameters T_pB and $T_p\Delta f$.

Chapter 5
Conclusion and Future work

5.1 Conclusion

Sidelobes in the spectrum of the radar signal is undesirable because of its potential to mask the smaller targets. They are meant to be minimized to a maximum level. This thesis looks into the various ways to find the minimum possible value of the sidelobes. Phase and Frequency modulation techniques to achieve the maximum value of PSLR is studied and simulated. Windowing or weighting of the received signal is done to suppress the sidelobes so that range resolution can be enhanced to acceptable level.

Barker coded signals produces lower sidelobes when processed adaptively and also they are more robust to operate in the noisy conditions.

Frequency stepping is also studied as it is one of the method to enlarge the overall bandwidth of the radar signal. It involves a number of narrow band pulses to achieve the goal. But, it is also associated with some ambiguous peaks, known as the 'grating lobes' which can be minimized by choosing proper design parameters of the signal. The stepped frequency LFM signal produces lower sidelobes if designed in a proper fashion but the mainlobe width becomes higher as they give more weightage to the center frequencies.

5.2 Future Work

Radar signal processing is one of the most diverse area of research. In future, I would like to work on some of the parametric measures to subsidize the sidelobes and maximize the range resolution of the system. Apart from barker coded signal and LFM, NLFM signal are interesting field of research. To diminish the complexity of the NLFM generation system is one of the area to work upon.

Besides these, I want to work on the processes involving the signals to make them more Doppler tolerant.

References

[1] Skolnik M., “Introduction to RADAR System”, TMH, 2001

[2] Levanon N., “RADAR Signals”, New York: Wiley, 2004.

[3] W. Siebert, “A Radar Detection Philosophy,” *IRE Trans.,* vol.IT-2, no. 3, pp. 204-221, Sept. 1956.

[4] C. Cook, “Radar signals: An introduction to theory and application”, Elsevier, 2012.

[5] L. R. Varshney and D. Thomas, “Sidelobe reduction for matched filter range processing”, in *Radar Conference, 2003. Proceedings of the 2003 IEEE,* 2003.

[6] Griffiths H. D. and Vinagre L., “Design Of low-sidelobe pulse compression waveforms”, Electronics Letters”, Vol. 30, pp. 1004-1005, 1994.

[7] M. N. Cohen, “An overview of high range resolution radar techniques”, in *Telesystems Conference, 1991. Proceedings. Vol. 1, NTC'91, National,* 1991.

[8] S. Salemian, M. Jamshihi and A. Rafiee, “Radar pulse compression techniques”, in *Proceedings of the 4th WSEAS international conference on Applications of electrical engineering,* 2005.

[9] Carpentier, Michel H., “Evolution of Pulse Compression in the Radar Field”, *Microwave Conference, 1979. 9th European,* vol., no., pp.45-53, 17-20 Sept. 1979.

[10] I. Gladkova, “Analysis of stepped-frequency pulse train design”, *Aerospace and Electronic Systems, IEEE Transactions on,* vol. 45, no. 4, pp. 1251-1261, 2009.

[11] E. Mozeson and N. Levanon, “MATLAB code for plotting ambiguity functions”, *IEEE Transactions on Aerospace and Electronic Systems,* vol. 38, no. 3, pp. 1064-1068, 2002.

[12] H.D. Griffiths and L.Vinagrae, “Design of low-sidelobe pulse compression waveforms,” *Electron Lett.,* vol.30, no.12, pp. 1004- 1005, June 1994.

[13] Ackroyd, M.H., and Ghani, F., “Optimum mismatch filters for sidelobe suppression”, *IEEE Trans. Aerosp. Electron. Syst*., pp. 214–218, 1973.

[14] Fu, J.S. and Xin Wu, “Sidelobe suppression using adaptive filtering techniques”, *in Proc. CIE International Conference on Radar,* pp.788-791, Oct. 2001.

[15] B. Zrnic, A. Zejak, A. Petrovic, and I. Simic, “Range sidelobe suppression for pulse compression radars utilizing modified RLS algorithm”, *in Proc. IEEE Int. Symp. Spread Spectrum Techniques and Applications*, Vol. 3, pp. 1008-1011, Sep 1998.

[16] M.N.Cohen, J.M. Baden, and P. E. Cohen, “Biphase Codes with Minimum Peak Sidelobe,” IEEE *International Radar Conf*, pp. 62-66, 1989.

[17] B. Widrow and S.D. Sterns, “Adaptive Signal Processing”, Prentice-Hall, Inc. Englewood Cliffs, New Jersey, 1985.

[18] S. Haykin, “*Adaptive Filter Theory*”, 4th edition, Pearson Education Asia, 2002.

[19] Fu, J.S. and Xin Wu, “Sidelobe suppression using adaptive filtering techniques”, *in Proc. CIE International Conference on Radar*, pp.788-791, Oct. 2001.

[20] B. Zrnic, A. Zejak, A. Petrovic, and I. Simic, “Range sidelobe suppression for pulse compression radars utilizing modified RLS algorithm”, *in Proc. IEEE Int. Symp. Spread Spectrum Techniques and Applications*, Vol. 3, pp. 1008-1011, Sep 1998.

[21] M. A. Richards, “Time and Frequency Domain Windowing OF LFM Pulses," 2006.

[22] R. J. Keeler and C.A. Hwang, “Pulse compression for weather radar”, *Radar Conference, Record of the IEEE 1995 International,* 1995

[23] K. Rajeswari, N. Gangatharan, E. Morris and G. Rao, “Sidelobe reduction techniques for range-resolution radar”, in *The 8th International Conference on Communication Systems,* Nov. 2002.

[24] A. K. Sahoo and G. Panda, “Sidelobe reduction of LFM signal using convolutional windows”, Proceedings of ICES Conference, pp. 86-89, 2011.

[25] Wang H., Shi J. and He J., “Compression with considerable sidelobe suppression effect in weather radar”, EURASIP Journal on Wireless Communications and Networking, 2013:97, 2013.

[26] Archana M. and Gnanpriya M., “Low power LFM pulse compression Radar with sidelobe suppression”, International Journal of Advanced Research in Electrical, Electronics and Instrumentation Engineering, Vol. 3, Issue 7, pp. 10672-10679, July 2014.

[27] I. Gladkova, “Analysis of stepped-frequency pulse train design”, *Aerospace and Electronic Systems, IEEE Transactions on,* vol. 45, no. 4, pp. 1251-1261, 2009.

[28] I. Gladkova and D. Chebanov, “Grating lobes suppression in stepped-frequency pulse train”, *Aerospace and Electronic Systems, IEEE Transactions on,* vol. 44, no. 4, pp. 1265-1275, 2008

[29] D. Chebanov, I. Gladkova and J. Weber, “Family of stepped-frequency LFM trains with low autocorrelation sidelobes”, in *Proceedings of the Second IASTED International Conference on Antennas, Radar and Wave Propagation*, 2005.

[30] N. Levanon and E. Mozeson, “Nullifying ACF grating lobes in stepped-frequency train of LFM pulses”, *Aerospace and Electronic Systems, IEEE Transactions on,* vol. 39, no. 2, pp. 694-703, 2003.

[31] A. K. Sahoo and G. Panda, "A multiobjective optimization approach to determine the parameters of stepped frequency pulse train", *Aerospace science and technology,* vol. 24, no. 1, pp. 101-110, 2013.